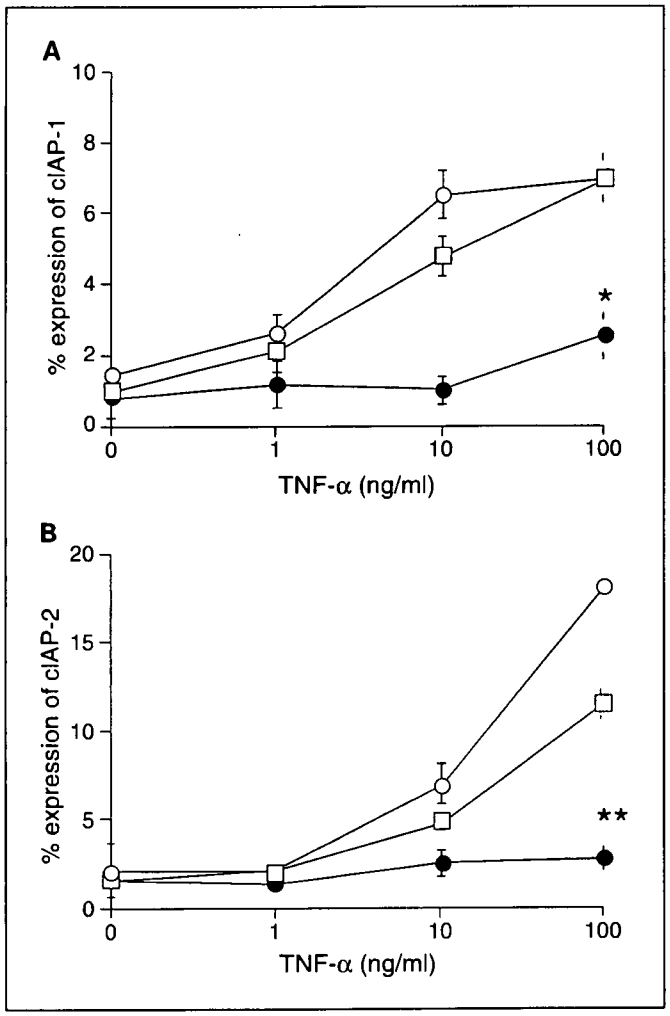

Fig. 5. TNF-α induced c-IAP1 and c-IAP2 mRNA expression in PC-9 and PC-9/ZD2001R cells but not in PC-9/ZD2001 cells. The cells were exposed to the indicated concentrations of TNF-α for 12 hours; after which mRNA was isolated with the guanidium isothiocyanate method. Induction of c-IAP1 (*A*) and c-IAP2 (*B*) mRNA was measured with a fluorescence-based real-time RT-PCR method using specific primer sets (as described in Materials and Methods). The expression levels of c-IAP1 and c-IAP2 mRNA were significantly and dose-dependently increased by exposure to TNF-α in PC-9 and PC-9/ZD2001R cells but this enhancement was rarely observed in PC-9/ZD2001 cells. Results expressed as the percentage of each cell line compared with the internal control, expression of β-actin mRNA. ○, PC-9; ●, PC-9/ZD2001; □, PC-9/ZD2001R. Points, mean of three different experiments; bars, SD. *, $P < 0.001$.

no data to explain the discrepancy between transforming growth factor-α-mediated and TNF-α-mediated EGFR signaling in this cell line. Nevertheless, TNF-α-mediated cross-talk signaling to EGFR, although ligand independent, seems to cause downstream activation in a different way from that caused through ligand-mediated direct EGFR activation. Akt/NF-κB signaling is also known to be downstream of other receptors, such as other Her family receptors (36), platelet-derived growth factor receptor (37), and IFN receptor (38). We previously confirmed the expression of other Her family receptors, Her2 and Her3, in PC-9 cells. Possibly, signaling of these receptors may be able to modulate the TNF-α-mediated cross-talk signaling and Akt/NF-κB signaling. Various aspects of TNF-α-induced cross-talk signaling to EGFR, such as EGFR heterodimer formation with other Her family receptors and downstream signaling specificity, require further investigation.

Human IAPs, c-IAP1 and c-IAP2, have been reported to block the apoptotic events caused by caspase-8 activation by directly combining with caspase-3 and caspase-7 and restraining them (10, 27). IAPs play a key role in the resistance to apoptotic effect of TNF-α superfamily of proteins (39) and various anticancer drugs (40, 41); for this reason, IAPs are considered promising targets in anticancer therapy (42, 43). To evaluate TNF-α-mediated antiapoptotic signaling, we measured IAP induction in these cell lines by means of Western blotting analysis and real-time RT-PCR. As might be expected, IAPs and their mRNAs were markedly induced by TNF-α in PC-9 and PC-9/ZD2001R cells but not in PC-9/ZD2001 cells (Fig. 5A and B). TNF-α-induced activation of caspase-3, but rarely of caspase-8, was significantly lower in PC-9 and PC-9/ZD2001R as compared with PC-9/ZD2001 (Fig. 3A and B). These results suggest that TNF-α precisely activates apoptotic signaling through caspase-8 in all three cell lines and that induction of IAPs blocks downstream signaling by inhibiting caspase-3 in PC-9 and PC-9/ZD2001R. In these cell lines, the induction of IAPs likely plays a key role in determining the sensitivity to TNF-α-mediated apoptosis among the antiapoptotic proteins that are induced by NF-κB-mediated transcription.

Several clinical studies of TNF-α as an anticancer treatment have been done, mainly in the 1970s; however, treatment with TNF-α was greatly limited by its side effects, particularly its toxicity to previously healthy organs (44–49). Recently, several new anticancer therapies using TNF-α have been developed, such as RGD-V29 (F4614) and TNF-erade (Biologic), in an attempt to reduce adverse effects (8, 9, 50, 51). We have shown that a NSCLC cell line with acquired resistance to gefitinib acquired collateral sensitivity to TNF-α. These data strongly suggest that treatment with TNF-α might be effective against tumors that have acquired resistance to gefitinib after long-term administration of this drug. Further analysis is required before clinical application.

In summary, the cross-talk signaling from TNFR to EGFR and subsequent IAP induction play important roles in the resistance to TNF-α-induced apoptosis in PC-9 cells. Because this signaling cascade is decreased in the gefitinib-resistant PC-9/ZD2001 cells, TNF-α did not activate the Akt/NF-κB cascade. This decrease of EGFR signaling to Akt/NF-κB pathway, which is related to gefitinib-acquired resistance, may contribute to the acquisition of hypersensitivity to TNF-α in this cell line.

References

1. Fukuoka M, Yano S, Giaccone G, et al. Multi-institutional randomized phase II trial of gefitinib for previously treated patients with advanced non-small-cell lung cancer (The IDEAL 1 Trial) [corrected]. J Clin Oncol 2003;21:2237–46.
2. Kris MG, Natale RB, Herbst RS, et al. Efficacy of gefitinib, an inhibitor of the epidermal growth factor receptor tyrosine kinase, in symptomatic patients with non-small cell lung cancer: a randomized trial. JAMA 2003;290:2149–58.
3. Kobayashi S, Boggon TJ, Dayaram T, et al. EGFR mutation and resistance of non-small-cell lung cancer to gefitinib. N Engl J Med 2005;352:786–92.
4. Pao W, Miller VA, Politi KA, et al. Acquired resistance of lung adenocarcinomas to gefitinib or erlotinib is associated with a second mutation in the EGFR kinase domain. PLoS Med 2005;2:e73.
5. Ashkenazi A. Targeting death and decoy receptors of the tumour-necrosis factor superfamily. Nat Rev Cancer 2002;2:420–30.
6. Basile JR, Zacny V, Munger K. The cytokines tumor

necrosis factor-α (TNF-α) and TNF-related apoptosis-inducing ligand differentially modulate proliferation and apoptotic pathways in human keratinocytes expressing the human papillomavirus-16 E7 oncoprotein. J Biol Chem 2001;276:22522–8.
7. Chen G, Goeddel Dv. TNF-R1 signaling: a beautiful pathway. Science 2002;296:1634–5.
8. Mundt AJ, Vijayakumar S, Nemunaitis J, et al. A Phase I trial of TNFerade biologic in patients with soft tissue sarcoma in the extremities. Clin Cancer Res 2004;10:5747–53.
9. Senzer N, Mani S, Rosemurgy A, et al. TNFerade biologic, an adenovector with a radiation-inducible promoter, carrying the human tumor necrosis factor α gene: a phase I study in patients with solid tumors. J Clin Oncol 2004;22:592–601.
10. Deveraux QL, Roy N, Stennicke HR, et al. IAPs block apoptotic events induced by caspase-8 and cytochrome *c* by direct inhibition of distinct caspases. EMBO J 1998;17:2215–23.
11. Roy N, Deveraux QL, Takahashi R, Salvesen GS, Reed JC. The c-IAP-1 and c-IAP-2 proteins are direct inhibitors of specific caspases. EMBO J 1997;16:6914–25.
12. Sidoti-De Fraisse C, Rincheval V, Risler Y, Mignotte B, Vayssiere JL. TNF-α activates at least two apoptotic signaling cascades. Oncogene 1998;17:1639–51.
13. Cappuzzo F, Magrini E, Ceresoli GL, et al. Akt phosphorylation and gefitinib efficacy in patients with advanced non-small-cell lung cancer. J Natl Cancer Inst 2004;96:1133–41.
14. Kulik G, Carson JP, Vomastek T, et al. Tumor necrosis factor α induces BID cleavage and bypasses antiapoptotic signals in prostate cancer LNCaP cells. Cancer Res 2001;61:2713–9.
15. Liu ZG, Hsu H, Goeddel DV, Karin M. Dissection of TNF receptor 1 effector functions: JNK activation is not linked to apoptosis while NF-κB activation prevents cell death. Cell 1996;87:565–76.
16. Argast GM, Campbell JS, Brooling JT, Fausto N. Epidermal growth factor receptor transactivation mediates tumor necrosis factor-induced hepatocyte replication. J Biol Chem 2004;279:34530–6.
17. Chen WN, Woodbury RL, Kathmann LE, et al. Induced autocrine signaling through the epidermal growth factor receptor contributes to the response of mammary epithelial cells to tumor necrosis factor α. J Biol Chem 2004;279:18488–96.
18. Hirota K, Murata M, Itoh T, Yodoi J, Fukuda K. Redox-sensitive transactivation of epidermal growth factor receptor by tumor necrosis factor confers the NF-κ B activation. J Biol Chem 2001;276:25953–8.
19. Izumi H, Ono M, Ushiro S, Kohno K, Kung HF, Kuwano M. Cross talk of tumor necrosis factor-α and epidermal growth factor in human microvascular endothelial cells. Exp Cell Res 1994;214:654–62.
20. Wang D, Yang EB, Cheng LY. Modulation of EGF receptor by tumor necrosis factor-α in human hepatocellular carcinoma HepG2 cells. Anticancer Res 1996;16:3001–6.
21. Woodworth CD, Mcmullin E, Iglesias M, Plowman GD. Interleukin 1 α and tumor necrosis factor α stimulate autocrine amphiregulin expression and proliferation of human papillomavirus-immortalized and carcinoma-derived cervical epithelial cells. Proc Natl Acad Sci U S A 1995;92:2840–4.
22. Beg AA, Baltimore D. An essential role for NF-κB in preventing TNF-α-induced cell death. Science 1996;274:782–4.
23. Wang CY, Mayo MW, Baldwin AS, Jr. TNF-and cancer therapy-induced apoptosis: potentiation by inhibition of NF-κB. Science 1996;274:784–7.
24. Wang CY, Guttridge DC, Mayo MW, Baldwin AS, Jr. NF-κB induces expression of the Bcl-2 homologue A1/Bfl-1 to preferentially suppress chemotherapy-induced apoptosis. Mol Cell Biol 1999;19:5923–9.
25. Mora AL, Corn RA, Stanic AK, et al. Antiapoptotic function of NF-κB in T lymphocytes is influenced by their differentiation status: roles of Fas, c-FLIP, and Bcl-xL. Cell Death Differ 2003;10:1032–44.
26. Kane LP, Shapiro VS, Stokoe D, Weiss A. Induction of NF-κB by the Akt/PKB kinase. Curr Biol 1999;9:601–4.
27. Rothe M, Pan MG, Henzel WJ, Ayres TM, Goeddel DV. The TNFR2-TRAF signaling complex contains two novel proteins related to baculoviral inhibitor of apoptosis proteins. Cell 1995;83:1243–52.
28. Wang CY, Mayo MW, Korneluk RG, Goeddel DV, Baldwin AS, Jr. NF-κB antiapoptosis: induction of TRAF1 and TRAF2 and c-IAP1 and c-IAP2 to suppress caspase-8 activation. Science 1998;281:1680–3.
29. Hoffmann M, Schmidt M, Wels W. Activation of EGF receptor family members suppresses the cytotoxic effects of tumor necrosis factor-α. Cancer Immunol Immunother 1998;47:167–75.
30. Lynch TJ, Bell DW, Sordella R, et al. Activating mutations in the epidermal growth factor receptor underlying responsiveness of non-small-cell lung cancer to gefitinib. N Engl J Med 2004;350:2129–39.
31. Paez JG, Janne PA, Lee JC, et al. EGFR mutations in lung cancer: correlation with clinical response to gefitinib therapy. Science 2004;304:1497–500.
32. Bianco R, Shin I, Ritter CA, et al. Loss of PTEN/MMAC1/TEP in EGF receptor-expressing tumor cells counteracts the antitumor action of EGFR tyrosine kinase inhibitors. Oncogene 2003;22:2812–22.
33. Ono M, Hirata A, Kometani T, et al. Sensitivity to gefitinib (Iressa, ZD1839) in non-small cell lung cancer cell lines correlates with dependence on the epidermal growth factor (EGF) receptor/extracellular signal-regulated kinase 1/2 and EGF receptor/Akt pathway for proliferation. Mol Cancer Ther 2004;3:465–72.
34. Sordella R, Bell DW, Haber DA, Settleman J. Gefitinib-sensitizing EGFR mutations in lung cancer activate anti-apoptotic pathways. Science 2004;305:1163–7.
35. Arao T, Fukumoto H, Takeda M, Tamura T, Saijo N, Nishio K. Small in-frame deletion in the epidermal growth factor receptor as a target for ZD6474. Cancer Res 2004;64:9101–4.
36. Prenzel N, Fischer OM, Streit S, Hart S, Ullrich A. The epidermal growth factor receptor family as a central element for cellular signal transduction and diversification. Endocr Relat Cancer 2001;8:11–31.
37. Rosenkranz S, Kazlauskas A. Evidence for distinct signaling properties and biological responses induced by the PDGF receptor α and β subtypes. Growth Factors 1999;16:201–16.
38. Uddin S, Fish EN, Sher DA, Gardziola C, White MF, Platanias LC. Activation of the phosphatidylinositol 3-kinase serine kinase by IFN-α. J Immunol 1997;158:2390–7.
39. Li L, Thomas RM, Suzuki H, De Brabander JK, Wang X, Harran PG. A small molecule Smac mimic potentiates TRAIL- and TNFα-mediated cell death. Science 2004;305:1471–4.
40. Ferreira CG, Van Der Valk P, Span SW, et al. Assessment of IAP (inhibitor of apoptosis) proteins as predictors of response to chemotherapy in advanced non-small-cell lung cancer patients. Ann Oncol 2001;12:799–805.
41. Vaziri SA, Grabowski DR, Tabata M, et al. c-IAP1 is overexpressed in HL-60 cells selected for doxorubicin resistance: effects on etoposide-induced apoptosis. Anticancer Res 2003;23:3657–61.
42. De Graaf AO, De Witte T, Jansen JH. Inhibitor of apoptosis proteins: new therapeutic targets in hematological cancer? Leukemia 2004;18:1751–9.
43. Nachmias B, Ashhab Y, Ben-Yehuda D. The inhibitor of apoptosis protein family (IAPs): an emerging therapeutic target in cancer. Semin Cancer Biol 2004;14:231–43.
44. Blick M, Sherwin SA, Rosenblum M, Gutterman J. Phase I study of recombinant tumor necrosis factor in cancer patients. Cancer Res 1987;47:2986–9.
45. Chapman PB, Lester TJ, Casper ES, et al. Clinical pharmacology of recombinant human tumor necrosis factor in patients with advanced cancer. J Clin Oncol 1987;5:1942–51.
46. Creaven PJ, Brenner DE, Cowens JW, et al. A phase I clinical trial of recombinant human tumor necrosis factor given daily for five days. Cancer Chemother Pharmacol 1989;23:186–91.
47. Feinberg B, Kurzrock R, Talpaz M, Blick M, Saks S, Gutterman JU. A phase I trial of intravenously-administered recombinant tumor necrosis factor-α in cancer patients. J Clin Oncol 1988;6:1328–34.
48. Gamm H, Lindemann A, Mertelsmann R, Herrmann F. Phase I trial of recombinant human tumour necrosis factor α in patients with advanced malignancy. Eur J Cancer 1991;27:856–63.
49. Spriggs DR, Sherman ML, Michie H, et al. Recombinant human tumor necrosis factor administered as a 24-hour intravenous infusion. A phase I and pharmacologic study. J Natl Cancer Inst 1988;80:1039–44.
50. Kuroda K, Miyata K, Fujita F, et al. Human tumor necrosis factor-α mutant RGD-V29 (F4614) shows potent antitumor activity and reduced toxicity against human tumor xenografted nude mice. Cancer Lett 2000;159:33–41.
51. Kuroda K, Miyata K, Tsutsumi Y, et al. Preferential activity of wild-type and mutant tumor necrosis factor-α against tumor-derived endothelial-like cells. Jpn J Cancer Res 2000;91:59–67.

Element Array by Scanning X-ray Fluorescence Microscopy after *Cis*-Diamminedichloro-Platinum(II) Treatment

Mari Shimura,[1] Akira Saito,[4,8,9] Satoshi Matsuyama,[5] Takahiro Sakuma,[1] Yasuhito Terui,[3] Kazumasa Ueno,[5] Hirokatsu Yumoto,[5] Kazuto Yamauchi,[5] Kazuya Yamamura,[6] Hidekazu Mimura,[5] Yasuhisa Sano,[5] Makina Yabashi,[7] Kenji Tamasaku,[8] Kazuto Nishio,[2] Yoshinori Nishino,[8] Katsuyoshi Endo,[6] Kiyohiko Hatake,[3] Yuzo Mori,[6] Yukihito Ishizaka,[1] and Tetsuya Ishikawa[8]

[1]Department of Intractable Diseases, International Medical Center of Japan; [2]Pharmacology Division, National Cancer Center Research Institute; [3]Division of Clinical Chemotherapy, Cancer Chemotherapy Center, Japanese Foundation for Cancer Research, Tokyo, Japan; Departments of [4]Material and Life Science and [5]Precision Science and Technology, and [6]Research Center for Ultra-Precision Science and Technology, Graduate School of Engineering, Osaka University, Suita, Osaka, Japan; [7]SPring-8/Japan Synchrotron Radiation Research Institute and [8]SPring-8/Riken, Hyogo, Japan; and [9]Nanoscale Quantum Conductor Array Project, ICORP, Saitama, Japan

Abstract

Minerals are important for cellular functions, such as transcription and enzyme activity, and are also involved in the metabolism of anticancer chemotherapeutic compounds. Profiling of intracellular elements in individual cells could help in understanding the mechanism of drug resistance in tumors and possibly provide a new strategy of anticancer chemotherapy. Using a recently developed technique of scanning X-ray fluorescence microscopy (SXFM), we analyzed intracellular elements after treatment with *cis*-diamminedichloro-platinum(II) (CDDP), a platinum-based anticancer agent. The images obtained by SXFM (element array) revealed that the average Pt content of CDDP-resistant cells was 2.6 times less than that of sensitive cells, and the zinc content was inversely correlated with the intracellular Pt content. Data suggested that Zn-related detoxification is responsible for resistance to CDDP. Of Zn-related excretion factors, glutathione was highly correlated with the amount of Zn. The combined treatment of CDDP and a Zn(II) chelator resulted in the incorporation of thrice more Pt with the concomitant down-regulation of glutathione. We propose that the generation of an element array by SXFM opens up new avenues in cancer biology and treatment. (Cancer Res 2005; 65(12): 4998-5002)

Introduction

Cis-Diamminedichloro-platinum(II) (CDDP) is an effective anticancer agent, but tumor cells can become resistant after CDDP-based therapy (1). Detoxification of CDDP, an increase in DNA repair, and excretion of CDDP have been implicated as major factors contributing to CDDP resistance (1). Incorporated CDDP is excreted by several molecules, such as overexpressed P-glycoprotein (2), a zinc-related defense system that is regulated by increased intracellular glutathione (GSH; ref. 3), and the ATP-dependent glutathione S-conjugate export pump (GS-X pump), which plays a role in the vesicle-mediated excretion of GSH-CDDP conjugates from resistant cells (4). Recent reports suggest that minerals such as zinc (Zn) and copper (Cu), important for normal cellular functions (5), are involved in CDDP resistance (6, 7). The simultaneous monitoring of multiple numbers of cellular elements would be helpful in identifying the mechanism of drug resistance in a malignant cell. The recently developed technique of scanning X-ray fluorescence microscopy (SXFM; refs. 8, 9) has made it possible to detect elements of interest by a single measurement and give a profile of these elements at the single-cell level (termed an element array). To examine the efficacy of element array analysis, we analyzed elements before and after treatment with CDDP and compared the element profiles of CDDP-sensitive and CDDP-resistant cells. We showed that the Zn content has an inverse correlation with Pt incorporation owing to a positive linkage with glutathione (GSH), a Zn-dependent detoxification factor. The combined treatment with CDDP and *N,N,N,N*-tetrakis-(2-pyridylmethyl)-ethylenediamine (TPEN), a Zn (II)-chelator (10), increased Pt uptake with a concomitant reduction of intracellular GSH. We propose that the element array is a versatile method suitable for obtaining information about metals involved in drug metabolism and could contribute to a novel strategy for anticancer chemotherapy.

Materials and Methods

Element array analysis by scanning X-ray fluorescence microscopy. SXFM was set up at an undulator beamline, BL29XU, of the SPring-8 synchrotron radiation facility (11) by combining a Kirkpatrick-Baez–type X-ray focusing system (12, 13), an XY-scanning stage for sample mounting, and an energy-dispersive X-ray detector (SDD, Röntec, Co., Ltd.). Monochromatic X-rays at 15 keV for Pt *L*-line excitation were focused into a 1.5 μm (*H*) × 0.75 μm (*W*) spot with a measured flux of ~ 1×10^{11} photons/s. The focused X-rays simultaneously yielded the fluorescence of various chemical species in a small volume of sample cells, as shown in Fig. 1*A*. The fluorescence from each element was taken independently and did not overlap except for the Pt$L\alpha$ signal, which was contaminated by Zn$K\beta$ (Fig. 1*A*). This was corrected by subtraction, as described previously (8). In this study, we could also measure Pt$L\beta$ as a unique signal of Pt (Fig. 1*A*). After counts were collected for 4.0 to 8.5 seconds at each pixel of scanning, the detected counts were normalized by incident beam intensity. In addition to the mapping images, an elemental concentration per single cell was calculated from the integrated elemental intensity over the whole mapping image.[10]

Requests for reprints: Yukihito Ishizaka, Department of Intractable Diseases, International Medical Center of Japan, 1-21-1 Toyama, Shinjuku-ku, 162-8655 Tokyo, Japan. Phone/Fax: 81-3-5272-7527; E-mail: zakay@ri.imcj.go.jp.

[10] A. Saito et al., manuscript in preparation.

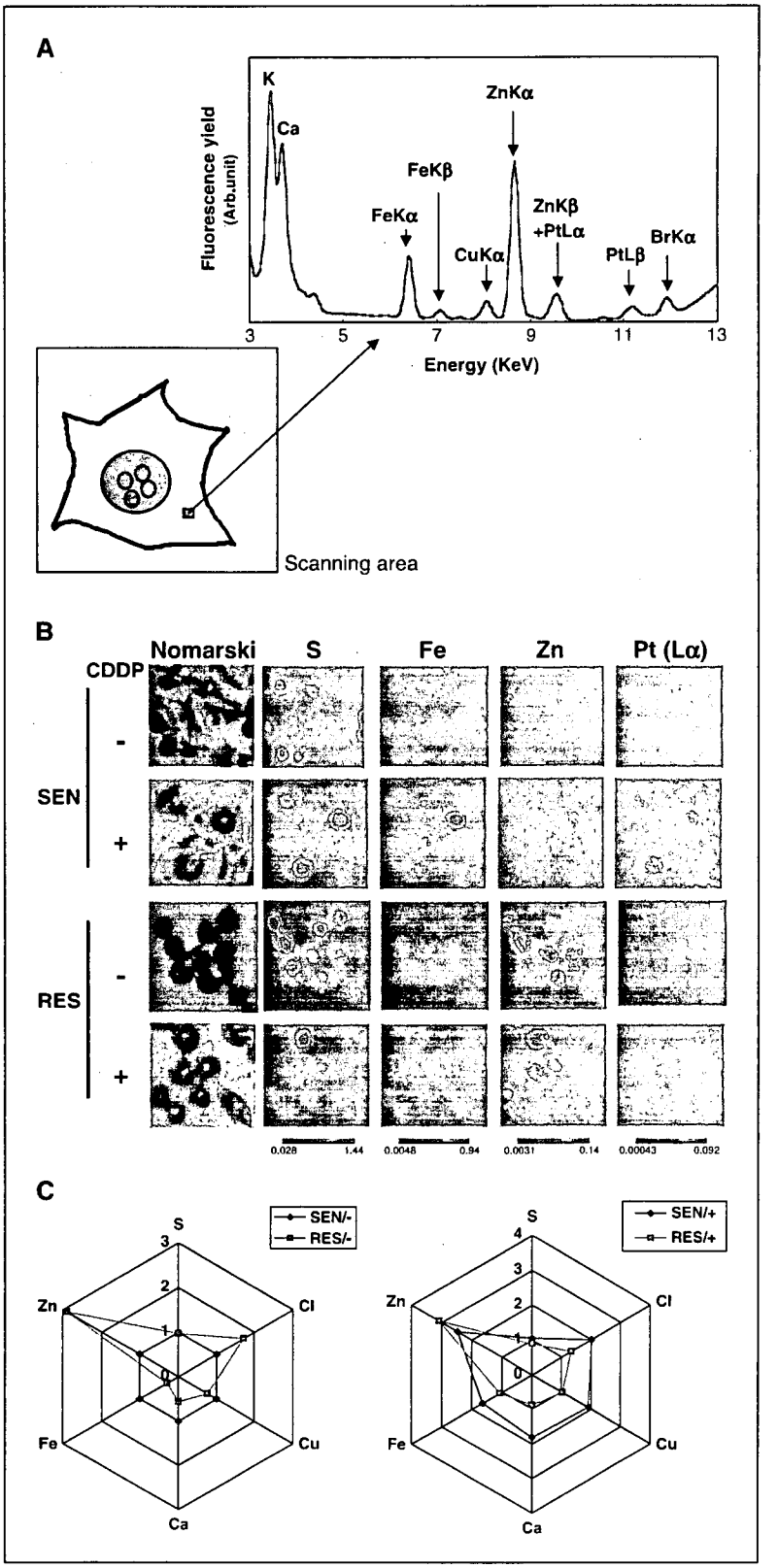

Figure 1. Element array by SXFM. *A,* scheme of imaging cellular elements by SXFM. Coherent X-rays are focused on each area (*pixel*), and the X-ray fluorescence from each element is detected. Each pixel gives an elemental spectrum, as shown in the right panel, and an integrated intensity of the individual element was mapped to the corresponding area of analyzed cells. *B,* SXFM analysis after CDDP treatment. Cell morphologies obtained by Nomarski are shown at ×100 magnification (*left*). Each field of view is equivalent to an area of 70 × 70 μm. Representative results are shown. Brighter colors indicate a higher signal intensity of each element. Results are shown for PC/SEN (*top*) and PC/RES cells (*bottom*). Note the high intensity of Pt*Lα* in PC/SEN cells after CDDP treatment (*second panel of the Pt column*) and the higher signal intensity of Zn in PC/RES cells compared with that of PC/SEN cells. *C,* element array based on SXFM analysis. The mean signal intensity of each element obtained by SXFM analysis was calculated, and the fold increase of elements in PC/RES cells (*red*) was depicted by using the intensity in PC/SEN cells (*blue*) as a standard (*left*). A part of analyzed elements is shown. The fold increase of elements in PC/SEN (*blue*) and PC/RES cells (*red*) after CDDP treatment was also shown by using the intensity in PC/SEN before CDDP treatment as a standard (*right*).

Chemicals and biochemical assays. TPEN (Sigma, St. Louis, MO; ref. 10), GSH (Calbiochem, La Jolla, CA), and CDDP (Daiichi Kagaku, Tokyo, Japan) were purchased. A GSH colorimetric assay kit (Calbiochem) and a BCA protein assay kit (Bio-Rad, Hercules, CA) were used for measuring intracellular GSH. About 3×10^5 to 4×10^5 cells were subjected to GSH measurement, and the data were normalized by cell number.

Cell lines. PC-9 cells (PC/SEN) and PC-9 cells resistant to CDDP (PC/RES), originally derived from a lung carcinoma cell line (14), were

maintained in DMEM (Nissui, Co., Tokyo, Japan) supplemented with 10% FCS (Sigma). The viability of PC/SEN cultured for 72 hours in the presence of 1 μmol/L CDDP was 40%, whereas that of PC/RES was ~90%. In this study, each cell line when treated with 1 μmol/L CDDP for 24 hours showed >85% viability.

Colony formation. After treatment, aliquots of PC/SEN and PC/RES were plated into culture dishes or soft agar, and the numbers of cell aggregates consisting of >50 cells were counted. Each number was normalized by plating efficiency, and the mean and SD of the number of formed colonies were calculated.

Sample preparation. Cells were plated on a silicon nitride base (NTT Advanced Technology, Tokyo, Japan) 1 day before the experiment. After incubation for 24 hours in the presence of 1 μmol/L CDDP, the cells were washed with PBS, fixed in 2% paraformaldehyde in PBS for 10 minutes at room temperature, and incubated in cold 70% ethanol for 30 minutes. The cells were then placed in a 1:3 solution of glacial acetic acid and methanol for 10 minutes, washed with 70% alcohol, and dried overnight at room temperature.

Measurement of cellular platinum and zinc. To measure Pt and Zn, ~5 × 10^6 cells were subjected to inductively coupled plasma mass spectroscopy (ICP-MS; Toray Research Center, Shiga, Japan; ref. 15).

Statistical analysis. The Pearson product-moment correlation coefficient and Student's *t* test were used to evaluate statistical significance (16).

Results and Discussion

Incorporation of platinum and element array after *cis*-diamminedichloro-platinum(II) treatment. We analyzed intracellular elements by SXFM after CDDP treatment (Fig. 1*A*). At 12 hours after treatment with 1 μmol/L CDDP, the level of Pt was increased in PC/SEN cells, whereas little increase in the Pt level was seen in PC/RES cells (Fig. 1*B*). The intensity of Pt in PC/RES cells was 2.6-fold less than that in PC/SEN cells, as confirmed by the results of ICP-MS, which indicated that the amount of Pt in PC/RES cells (5.5 fg/cell) was 3.6-fold less than that in PC/SEN cells (19.7 fg/cell). Therefore, the decreased accumulation of CDDP is likely to be responsible for resistance in PC/RES cells.

Based on the mean signal intensity obtained by SXFM, element array analysis was carried out (Fig. 1*C*). The element profile

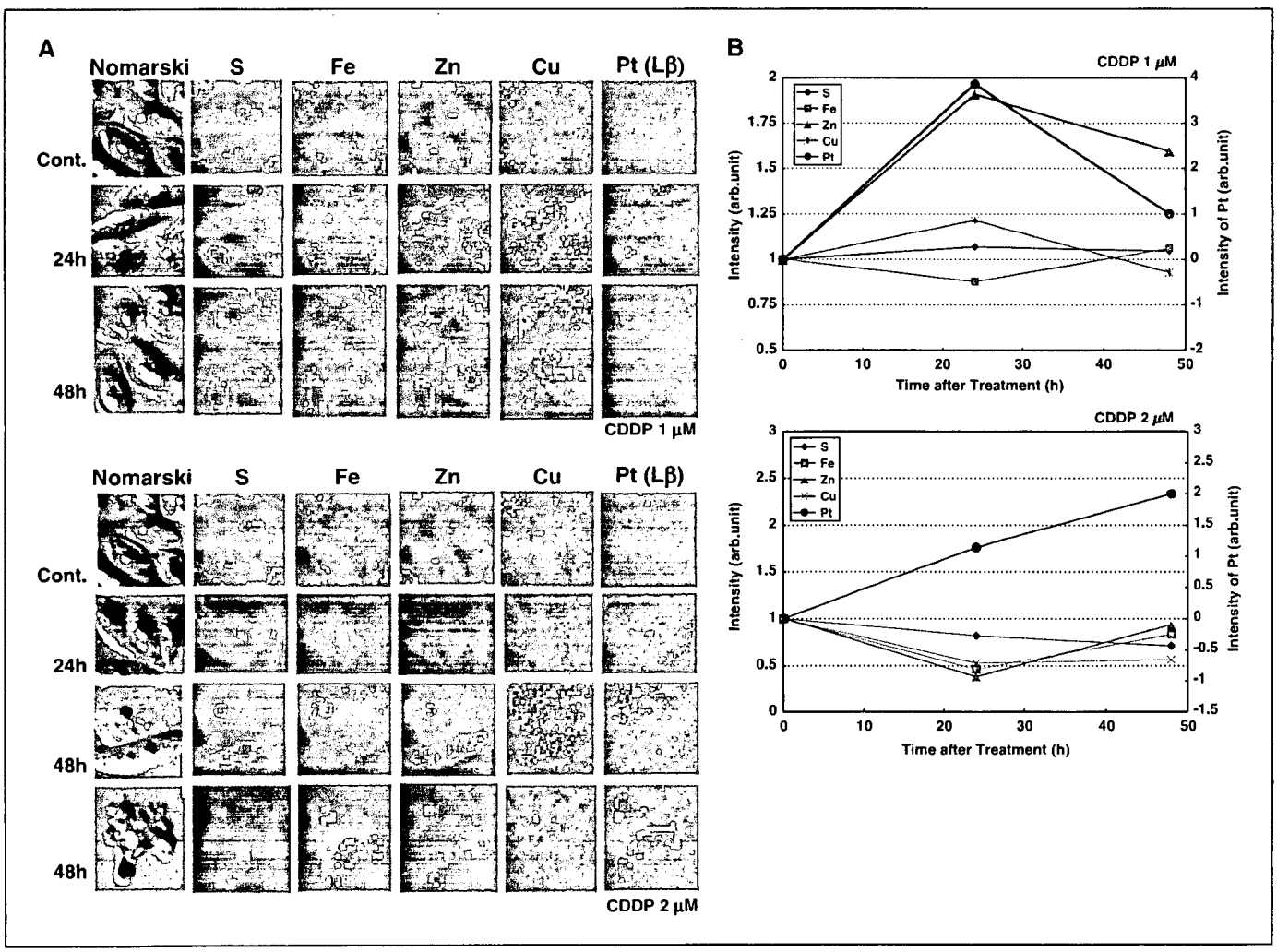

Figure 2. Chronological changes in elements after CDDP treatment. *A*, detection of elements in CDDP-treated PC/SEN cells. From the left, Nomarski images, signals of S, Fe, Zn, Cu, and Pt are shown. Top and bottom sets of panels show cells treated with 1 and 2 μmol/L CDDP, respectively. In each set of panels, control cells (*top*) and cells treated with CDDP for 24 hours (*middle*) and 48 hours (*bottom*) are shown. In this experiment, the signals of Pt*Lβ* were measured instead of Pt*Lα* (see Materials and Methods). The lowest panels show an apoptotic cell after 48 hours. *B*, summarized results of chronological changes of elements. The results after treatment with 1 μmol/L (*top*) and 2 μmol/L CDDP (*bottom*) are shown. The mean signal intensity was calculated from the results partly shown in (*A*). Among the cellular elements, Zn was most influenced by both 1 and 2 μmol/L CDDP treatment and had an inverse correlation with Pt content.

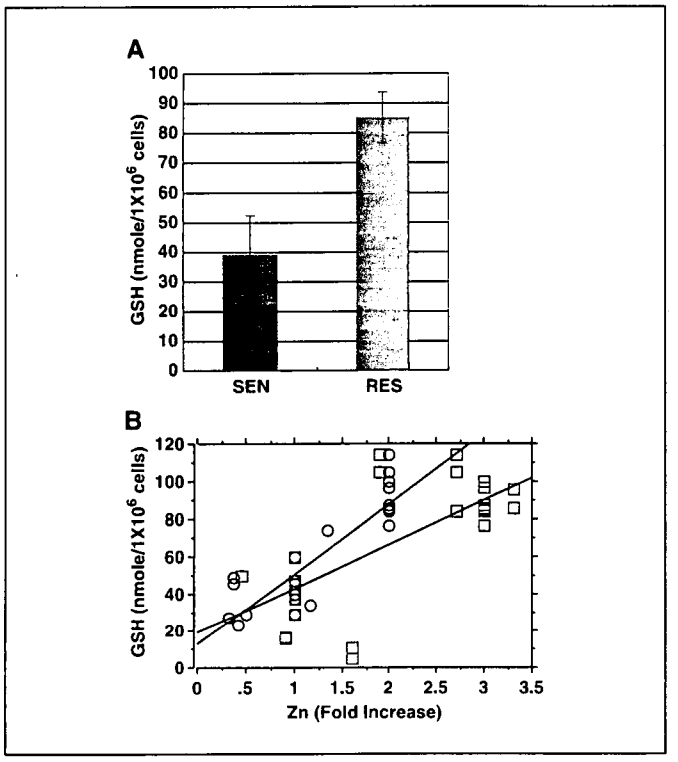

Figure 3. Cellular Zn content and GSH. *A*, basal level of intracellular GSH. The intracellular GSH levels in PC/SEN (*black*) and PC/RES cells (*gray*) were measured. GSH was significantly higher in PC/RES than in PC/SEN cells (*t* test, $P < 0.05$). *B*, correlation between Zn and intracellular GSH. A scatter diagram for Pearson product-moment correlation coefficient is depicted. Zn, measured by SXFM (*red squares*, $n = 27$) and by ICP-MS (*green circles*, $n = 29$), was plotted against intracellular GSH. Scattered values were based on data from both PC/SEN and PC/RES cells. The correlation coefficient r was calculated, and the statistical significance was determined ($P < 0.05$).

facilitates the identification of the elements related to the mechanism of drug resistance to CDDP. First, we noticed that the Zn content of untreated PC/RES cells was ~3-fold of that in PC/SEN cells (Fig. 1*C*, *left*). The difference in the Zn contents of these cells was confirmed by ICP-MS analysis (105 fg/cell for PC/SEN cells and 189 fg/cell for PC/RES cells, respectively). When 1 μmol/L CDDP was used for treatment, constitutive high Zn was observed in PC/RES (Fig. 1*C*, *right*). In PC/SEN cells, the amounts of all the elements were slightly increased, but the amount of Zn was increased most markedly.

We then analyzed the chronological changes in the levels of elements in PC/SEN cells following CDDP treatment. Representative results for S, Fe, Zn, Cu, and Pt are shown in Fig. 2*A*. Pt was clearly observed at 24 hours after treatment with 1 or 2 μmol/L CDDP (Fig. 2*A*). It was, however, barely detectable at 48 hours after the cells were treated with 1 μmol/L CDDP (Fig. 2*A*, *top*), suggesting that the cells excreted CDDP. In contrast, the cellular content of Pt gradually increased after treatment with 2 μmol/L CDDP (Fig. 2*A*, *bottom*), and apoptotic cells with high levels of incorporated CDDP were observed after 48 hours (Fig. 2*A*, *bottom*).

The element profile was plotted against the time after treatment with CDDP (Fig. 2*B*). When the cells were treated with 1 μmol/L CDDP, the Zn content increased remarkably and reached a peak at 24 hours (Fig. 2*B*, *top*, *red line*). In these cells, the Pt content was reduced after 48 hours. When the cells were treated with 2 μmol/L CDDP, the Zn content decreased within 24 hours (Fig. 2*B*, *bottom*), and the Pt content increased within 48 hours. In this analysis, Cu did not show significant changes. The results imply that the intracellular Zn content has an inverse correlation with the incorporated Pt content.

Cellular zinc and zinc-related detoxification. We studied Zn-related detoxification factors, such as metallothioneins (17), GSH (18), and the GSH-coupled excretory pump GS-X (4), and we observed that intracellular GSH was high in PC/RES cells (Fig. 3*A*). We then examined the possible correlation between the intracellular Zn content and GSH. As shown in Fig. 3*B*, the GSH levels showed a significant correlation with the levels of Zn detected by both ICP-MS and SXFM (Pearson product-moment correlation coefficient $r = 0.794$, $P < 0.05$ and $r = 0.533$, $P < 0.05$, respectively). The levels of Zn detected by SXFM may have less correlation with GSH than do the levels detected by ICP-MS because SXFM analyzed Zn in a small number of cells, whereas the analyses of GSH using ICP-MS were carried out on $>10^5$ cells.

Effects of zinc depletion and *cis*-diamminedichloroplatinum(II) uptake. To examine ways of increasing the sensitivity of PC/RES cells to CDDP, we used the Zn(II) chelator TPEN, as it was thought that CDDP uptake would increase when the GSH level was down-regulated by decreased Zn. Consistent with this hypothesis, treatment with 7.5 μmol/L of TPEN decreased cellular Zn to ~40 fg/cell at 30 hours after treatment in PC/SEN cells (Fig. 4*A*, *left*, *solid line*). The decrease seen in PC/RES cells owing to TPEN treatment was more rapid, with the Zn concentration being reduced to ~40 fg/cell within 7 hours (Fig. 4*A*, *left*, *dashed line*). The intracellular GSH also decreased with the reduction in intracellular Zn (Fig. 4*A*, *right*, *dashed line*).

To determine the effects of TPEN on the growth of PC/RES cells, the cells were pulse-treated for 2 hours with TPEN for 5 consecutive days and the growth was examined. Although treatment with 1 μmol/L CDDP did not induce apparent morphologic changes (Fig. 4*B*, *bottom*, *left*), the combined treatment with TPEN and CDDP caused prominent changes (Fig. 4*B*, *bottom*, *right*). A colony formation assay clearly showed that the combination of CDDP and TPEN, as well as single TPEN treatment, significantly impaired the growth of PC/RES cells (Fig. 4*C*). Consistent with these changes, ICP-MS indicated that the intracellular Pt content increased 3.5-fold after the combined treatment (from 0.38 to 1.35 fg/cell with TPEN treatment). It is important to note that the same dose of TPEN did not attenuate the growth of PC/SEN cells (Fig. 4*C*). These data indicate that the GSH level seems to be critical for resistance in PC/RES cells, consistent with previous reports that CDDP-resistant cells have high levels of GSH and that a decrease in GSH results in loss of resistance (3, 19). Our data also suggest that the high GSH content was maintained by the effects of Zn in PC/RES cells. Overall, our trial treatment with combined TPEN and CDDP suggests that this combination would be effective in eliminating tumors even if they include a CDDP-resistant population of cells with high Zn content.

We showed the use of element array analysis by SXFM to examine a mechanism of CDDP resistance. Based on element profiles, we successfully overcame CDDP resistance in PC/RES cells by using a Zn chelator that down-regulated the GSH level. Although it has been reported that Cu is a necessary factor for CDDP incorporation (7), the present work revealed that Cu was not involved in PC/RES cells. It is tempting to speculate that drug resistance is generated by various elements, and we propose that an element array can contribute to better understanding of cancer biology as well as other fields of medical science.

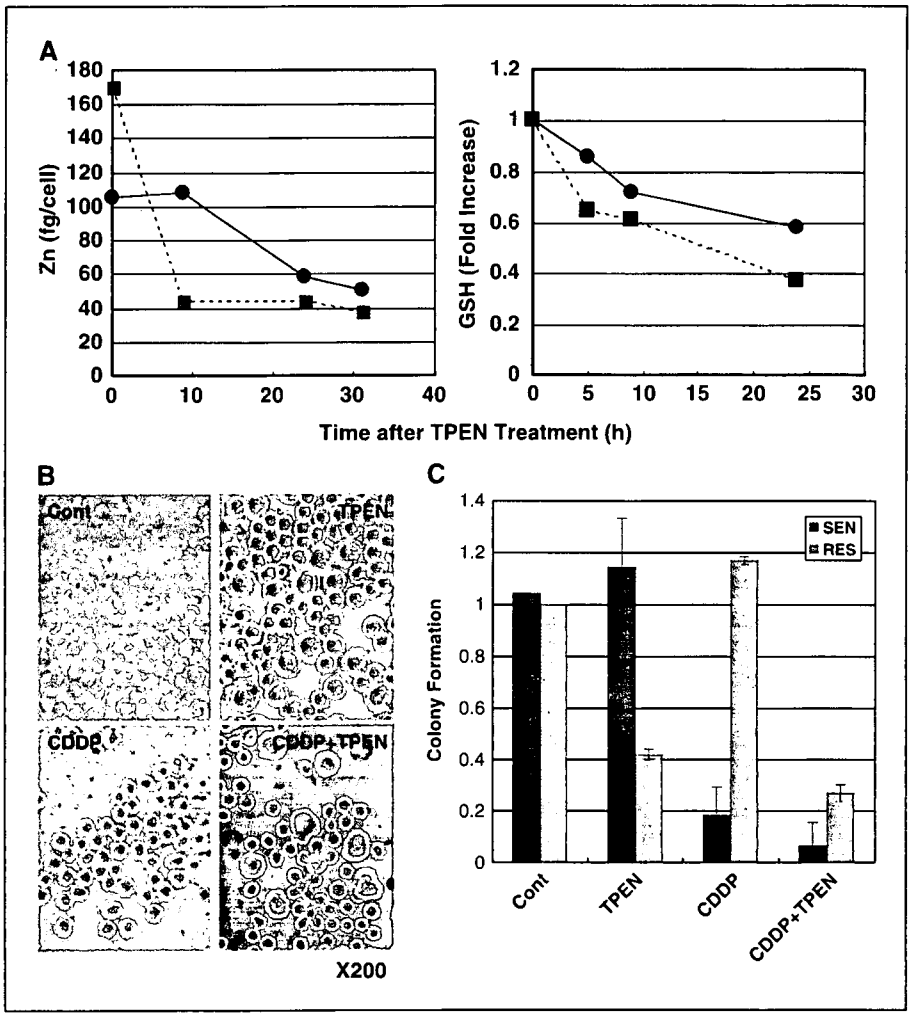

Figure 4. Cellular Zn content and Pt uptake with TPEN. *A*, TPEN-induced depletion of cellular Zn and down-regulation of GSH. TPEN (7.5 μmol/L) was added to the culture medium for the indicated time periods, and cellular Zn was measured by ICP-MS (*left*). Intracellular GSH content was also monitored (*right*). The Zn contents in PC/SEN (*solid lines*) and PC/RES cells (*dashed lines*) are shown. *B*, morphologic changes after pulse treatment with TPEN and CDDP. The morphologies of untreated PC/RES cells (*top*, *left*) and of cells treated with TPEN (*top*, *right*), CDDP (*bottom*, *left*), and CDDP plus TPEN (*bottom*, *right*) are shown. The cells were exposed to 1.0 μmol/L CDDP with or without 7.5 μmol/L TPEN for 2 hours, and then the medium was replaced with fresh medium. Pulse treatment was carried out for 5 consecutive days. Magnification, ×200. Note that large cells are observed after treatment with TPEN alone, and larger cells with irregular shape are observed following the combination treatment. The data showed that TPEN caused cellular accumulation at G_2-M phase with mitotic failure (data not shown). *C*, colony formation after pulse treatment with CDDP with or without TPEN. After pulse treatment for 5 consecutive days, as described in (*B*), the cells were plated in soft agar and the colony formation assay was done. The means and SDs of colony numbers of PC/SEN (*black columns*) and PC/RES cells (*gray columns*) are shown. The experiments were carried out in triplicate.

Acknowledgments

Received 2/3/2005; accepted 4/20/2005.

Grant support: Grant-in-aid for scientific research from the Ministry of Health, Labor, and Welfare of Japan and grant-in-aid for Center of Excellence Research (grant 08CE2004) from the Ministry of Education, Sports, Culture, Science, and Technology of Japan. The usage of BL29XU of the SPring-8 was supported by RIKEN.

The costs of publication of this article were defrayed in part by the payment of page charges. This article must therefore be hereby marked *advertisement* in accordance with 18 U.S.C. Section 1734 solely to indicate this fact.

We thank Harumi Shibata and Yasunori Suzuki for technical assistance.

References

1. Boulikas T, Vougiouka M. Cisplatin and platinum drugs at the molecular level. Oncol Rep 2003;10:1663–82.
2. Kuo TH, Liu FY, Chuang CY, Wu HS, Wang JJ, Kao A. To predict response chemotherapy using ^{99m}technetium tetrofosmin chest images in patients with untreated small cell lung cancer and compare with p-glycoprotein, multidrug resistance related protein-1, and lung resistance-related protein expression. Nucl Med Biol 2003;30:627–32.
3. Godwin AK, Meister A, O'Dwyer PJ, Huang CS, Hamilton TC, Anderson ME. High resistance to cisplatin in human ovarian cancer cell lines is associated with marked increase of glutathione synthesis. Proc Natl Acad Sci U S A 1992;89:3070–4.
4. Ishikawa T, Wright CD, Ishizuka H. GS-X pump is functionally overexpressed in *cis*-diamminedichloroplatinum (II)-resistant human leukemia HL-60 cells and down-regulated by cell differentiation. J Biol Chem 1994;269:29085–93.
5. Mayes PA, Nutrition. In: Murray RK, Granner DK, Mayers PA, Rodwell VW, editors. Harper's biochemistry. Chapter 54. 25th ed. New York: McGraw-Hill; 2000. p. 653–61.
6. Koropatnick J, Pearson J. Zinc treatment, metallothionein expression, and resistance to cisplatin in mouse melanoma cells. Somat Cell Mol Genet 1990;16:529–37.
7. Katano K, Kondo A, Safaei R, et al. Acquisition of resistance to cisplatin is accompanied by changes in the cellular pharmacology of copper. Cancer Res 2002;62:6559–65.
8. Ilinski P, Lai B, Cai Z, et al. The direct mapping of the uptake of platinum anticancer agents in individual human ovarian adenocarcinoma cells using a hard X-ray microprobe. Cancer Res 2003;63:1776–9.
9. Hall MD, Dillon CT, Zhang M, et al. The cellular distribution and oxidation state of platinum(II) and platinum(IV) antitumor complexes in cancer cells. J Biol Inorg Chem 2003;8:726–32.
10. Parat M-O, Richard M-J, Meplan C, Favir A, Béani J-C. Impairment of cultured cell proliferation and metallothionein expression by metal chelator *NNN′N′*-tetrakis-(2-pyridylmethyl)ethylene diamine. Biol Trace Elem Res 1999;70:51–68.
11. Miao J, Hodgson KO, Ishikawa T, Larabell CA, LeGros MA, Nishino Y. Imaging whole *Escherichia coli* bacteria by using single-particle X-ray diffraction. Proc Natl Acad Sci U S A 2003;100:110–2.
12. Kirkpatrick P, Baez AV. Formation of optical images by X-rays. J Opt Soc Am 1948;38:766–74.
13. Yamauchi K, Yamamura K, Mimura H, et al. Two-dimensional submicron focusing of hard X-rays by two elliptical mirrors fabricated by plasma chemical vaporization machining and elastic emission machining. Jpn J Appl Phys 2003;42:7129–34.
14. Kawamura-Akiyama Y, Kusaba H, Kanzawa F, Tamura T, Saijo N, Nishio K. Non-cross resistance of ZD0473 in acquired cisplatin-resistant lung cancer cell lines. Lung Cancer 2002;38:43–50.
15. Richarz AN, Wolf C, Bratter P. Determination of protein-bound trace elements in human cell cytosols of different organs and different pathological states. Analyst 2003;128:640–5.
16. Glantz SA. How to test for trends. In: Glantz SA, editor. Primer of biostatistics. Chapter 8. 2nd ed. New York: McGraw-Hill; 1987. p. 191–244.
17. Jourdan E, Jeanne RM, Régine S, Pascale G. Zinc-metallothinein genoprotective effect is independent of the glutathione depletion in HaCaT keratinocytes after solar light irradiation. J Cell Biochem 2004;92:631–40.
18. Parat M-O, Richard M-J, Béani J-C, Favier A. Involvement of zinc in intracellular oxidant/antioxidant balance. Biol Trace Elem Res 1997;60:187–204.
19. Hamaguchi K, Godwin AK, Yakushiji M, O'Dwyer PJ, Ozols RH, Hamilton TC. Cross-resistance to diverse drugs is associated with primary cisplatin resistance in ovarian cancer cell lines. Cancer Res 1993;53:5225–32.

British Journal of Cancer (2005) 92, 1877–1880

www.bjcancer.com

Gefitinib treatment affects androgen levels in non-small-cell lung cancer patients

M Nishio*[,1], F Ohyanagi[1], A Horiike[1], Y Ishikawa[3], Y Satoh[2], S Okumura[2], K Nakagawa[2], K Nishio[4] and T Horai[1]

[1]Division of Internal Medicine, Cancer Institute Hospital, Japanese Foundation For Cancer Research, Ariake 3-10-6, Koto-ku, Tokyo 135-8550, Japan; [2]Department of Chest Surgery, Cancer Institute Hospital, Japanese Foundation For Cancer Research, Tokyo, Japan; [3]Department of Pathology, Cancer Institute, Japanese Foundation For Cancer Research, Tokyo, Japan; [4]Pharmacology Division, National Cancer Center Research Institute, Tokyo, Japan

Gefitinib, an inhibitor of the epidermal growth factor receptor (EGFR, HER1/ErbB1) tyrosine kinase, has been shown to have clinical activity against non-small-cell lung cancers (NSCLCs), especially in women nonsmokers with adenocarcinomas. The aim of the present study was to clarify the relationship between androgen levels and gefitinib treatment in patients with advanced NSCLCs. Sera from 67 cases (36 men and 31 women) were obtained pretreatment and during treatment with gefitinib monotherapy (days 14–18) for examination of testosterone, dehydroepiandrosterone sulphate (DHEA), and dehydroepiandrosterone sulphate (DHEAS) levels. Testosterone and DHEA during treatment were significantly lower than the pretreatment values in both women and men, and the DHEAS levels during treatment were also significantly lowered in women. Gefitinib treatment significantly suppressed androgen levels, especially in women who had no smoking history. In addition, hormone levels in women responding to gefitinib were significantly lower during the treatment than in women who did not respond. Gefitinib-associated decrease in serum androgen levels may play a role in its clinical efficacy.
British Journal of Cancer (2005) **92,** 1877–1880. doi:10.1038/sj.bjc.6602585 www.bjcancer.com
Published online 3 May 2005

Keywords: sex hormone; epidermal growth factor receptor; tyrosine kinase inhibitor

Non-small-cell lung cancer (NSCLC) is a major health problem worldwide for both men and women (Ferlay *et al*, 2001). Usually at the time of diagnosis more than 50% of the patients have advanced or metastatic disease. While cytotoxic chemotherapy slightly prolongs survival among advanced NSCLC patients, it exerts clinically significant adverse effects (Non-Small-Cell Lung Cancer Collaborative Group, 1995; Schiller *et al*, 2002). An effective, palliative, low-toxicity treatment for patients with advanced NSCLC is therefore needed and for this purpose the epidermal growth factor receptor (EGFR/HER1) is a promising target. Gefitinib (ZD 1839, Iressa; AstraZeneca, London, UK) is an orally active, selective HER1-tyrosine kinase inhibitor (Wakeling *et al*, 2002), which has been shown to elicit objective responses in NSCLC cases, particularly in women nonsmokers with adenocarcinomas (Fukuoka *et al*, 2003; Kris *et al*, 2003). Recently, active mutations of EGFR have been identified in such cases (Paez *et al*, 2004; Pao *et al*, 2004) and may be linked with the sensitivity to gefitinib (Lynch *et al*, 2004; Paez *et al*, 2004; Pao *et al*, 2004). However, the reason why mutations frequently occur in these particular individuals is poorly understood.

Androgens are important hormones that play definitive roles in the differentiation of males and females. They can modify the activity of the epidermal growth factor network and EGFR signaling is essential for androgen-induced proliferation (Klein and Nielsen, 1993; Dammann *et al*, 2000; Torring *et al*, 2003). A receptor for androgens has been reported to occur in NSCLCs (Beattie *et al*, 1985; Kaiser *et al*, 1996) and there may be cooperative interaction between the hormones and active mutations of EGFR during the development of lung cancer. Previous reports have suggested that smoking increases the levels of androgens in men and women (Law *et al*, 1997; Trummer *et al*, 2002) and carcinogens from cigarette smoke may disrupt androgen function by reducing androgen receptor (AR) levels in androgen-responsive organs (Lin *et al*, 2004).

On the basis of these reports, we hypothesised that androgens may play an important role in the efficacy of gefitinib in NSCLC cases. In the present study, we therefore evaluated androgen levels in patients treated with gefitinib and the relationship with clinical efficacy.

PATIENTS AND METHODS

Between September 2002 and May 2004, 67 advanced or recurrent NSCLC patients were analysed in this study. All 67 were treated at our institution with gefitinib monotherapy (250 mg oral doses of gefitinib once daily) until disease progression occurred. Response evaluation and confirmation were performed in accordance with the WHO criteria (WHO, 1979). In brief, complete response (CR) was defined as complete disappearance of all lesions in imaging studies for at least 4 weeks without the appearance of any new lesions. Partial response (PR) was defined as a $>50\%$ decrease under the baseline in the sum of the products of the

*Correspondence: Dr M Nishio; E-mail: mnishio@jfcr.or.jp
Received 13 December 2004; revised 21 March 2005; accepted 21 March 2005; published online 3 May 2005

perpendicular diameters of all measurable lesions and at least stabilisation of all nonmeasurable lesions over a minimum period of 4 weeks. Progressive disease (PD) was defined as a >25% increase in the sum of the products of all measurable lesions, an unequivocal increase of nonmeasurable disease, or the appearance of new lesions. Cases were classified as having stable disease (SD) if none of the criteria for classifying responses as a CR, PR, or PD were met.

Blood was drawn before and during gefitinib administration. A previous report indicated the median time to symptom improvement with gefitinib to be only 8 days (Fukuoka *et al*, 2003), and we therefore checked the hormone levels at days 14–18, when serum was sampled between 10:00 and 14:00 and stored at 80°C for subsequent analyses. Serum levels of testosterone, dehydroepiandrosterone (DHEA), and dehydroepiandrosterone sulphate (DHEAS) were all measured at the SRL Laboratory (Tokyo, Japan). For testosterone, an electrochemiluminescence immunoassay was applied (ECLusys testosterone; Roche Diagnostics KK, Tokyo, Japan) and radioimmunoassays were used for DHEA and DHEAS (DPC DHEA and DPC DHEAS kits; Diagnostic Products Corporation, Los Angeles, CA, USA). The detection limits for testosterone, DHEA, and DHEAS were 5, 0.2, and 20 ng ml^{-1}, respectively. Inter- and intra-assay coefficients of variation were 6 and 8% for testosterone, 8 and 9% for DHEA, and 4 and 4% for DHEAS, respectively.

Appropriate ethical review boards approved the study, which followed the recommendations of the Declaration of Helsinki for biomedical research involving human subjects.

Statistical analysis

A paired *t*-test was used to compare the androgen levels between the two time periods. Patients were grouped into responders (CR and PR) and nonresponders (SD and PD) and the variables in each group were compared with an unpaired *t*-test. All statistical analyses were performed using SPSS version 8 statistical software (SPSS Inc., IL, USA).

RESULTS

Patient characterisation

Data for patient characteristics are listed in Table 1. Of the 67, 31 (46.3%) were women. The median age was 61 years (range, 42–80 years). There were 26 patients (38.8%) who had never smoked and adenocarcinoma was the primary histological finding in 56 cases (83.6%). There was no prior chemotherapy in 16 (23.9%) of the patients, and the remainder had received platinum-based chemotherapy.

Response to treatment could only be evaluated in 64 of the 67 cases. We observed 20 PR (29.8%), and of these, 13 (65%) were women and seven (35%) were men ($P=0.074$). The median and range of treatment duration with gefitinib were 2.1 and 0.2–21 months. In all, 10 (50%) of 20 responders and 29 (66%) of 44 nonresponders had a smoking history ($P=0.226$).

Effects of gefitinib treatment on androgens levels in NSCLC patients

Testosterone, DHEA, and DHEAS were detected in the serum of all 67 patients (see Table 2). There was a significant difference observed between men and women for serum testosterone levels ($P<0.0001$), but not for serum DHEA or DHEAS (DHEA; $P=0.267$, DHEAS; $P=0.0565$).

In women, testosterone, DHEA, and DHEAS levels at pretreatment were significantly higher than during treatment (testosterone; $P=0.025$, DHEA; $P=0.0065$, DHEAS; $P=0.0326$). In men, pretreatment testosterone and DHEA levels were significantly higher than during treatment, but there was no significant difference for DHEAS (testosterone, $P=0.0009$; DHEA, $P=0.0085$; DHEAS, $P=0.33$). In addition, we compared hormone levels between smokers and nonsmokers. Pretreatment, there were no significant differences between women with and without a smoking history. On the other hand, hormone levels were significantly suppressed by gefitinib treatment in the 21 women who had no smoking history (testosterone, $P=0.0016$; DHEA,

Table 1 Patient characteristics

Variable	No. of patients	%
Total	67	
Sex		
Male	36	53.7
Female	31	46.3
Age (years)		
Median	61	
Range	42–80	
Smoking history		
Never	26	38.8
Former/current	41	61.2
Performance status		
0, 1	48	71.6
>2	19	28.4
Histology		
Ad	56	83.6
Non-Ad	11	16.4
Stage		
II–III	17	25.4
IV	27	40.3
Recurrence after surgery	23	34.3
Response		
PR	20	29.8
SD/PD	44	64.7
NE	3	4.5
Prior chemotherapy		
No	16	23.9
Yes	51	76.1

Ad = adenocarcinoma; non-Ad = nonadenocarcinoma; PR = partial response; SD = stable disease; PD = progressive disease; NE = not evaluable.

Table 2 Androgen levels in patients treated with gefitinib

	Pretreatment		During treatment		
Variable	***n***	**Mean ± s.d.**	***n***	**Mean ± s.d.**	**Paired *t*-test**
Testosterone (ng ml^{-1})					
Female		21.5 ± 12.0	31	13.8.0 ± 11.0	$P=0.025$
Male	37	409.7 ± 129.8	37	350.8 ± 135.7	$P=0.0009$
DHEA (ng ml^{-1})					
Female	31	2.21 ± 2.03	31	1.33 ± 0.83	$P=0.0065$
Male	37	1.78 ± 1.06	37	1.49 ± 0.92	$P=0.0085$
DHEAS (ng ml^{-1})					
Female	31	854.4 ± 579.5	31	645.8 ± 365.6	$P=0.0326$
Male	37	1137.4 ± 607.7	37	1103.0 ± 601.5	$P=0.33$

s.d. = standard deviation; DHEA = dehydroepiandrosterone; DHEAS = dehydroepiandrosterone sulphate.

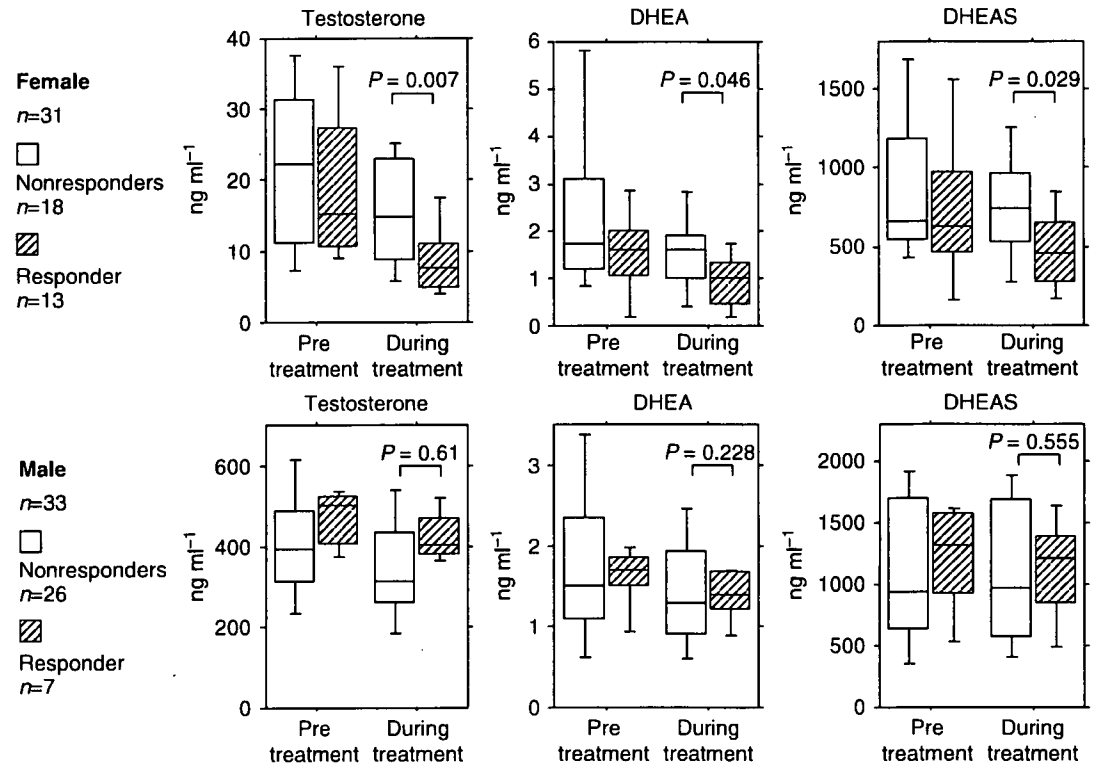

Figure 1 Serum testosterone, DHEA, and DHEAS levels, pretreatment and during the gefitinib administration. Each androgen levels are depicted in accordance to clinical response of gefitinib treatment (responders, PR; nonresponders, SD or PD). Error bars showed standard deviation.

$P=0.0157$; DHEAS, $P=0.0441$), but not in the 10 who had a smoking history (testosterone, $P=0.6159$; DHEA, $P=0.2487$; DHEAS, $P=0.4740$). Figure 1 depicts the androgen levels for women after dividing the group into responders *vs* nonresponders. Testosterone, DHEA, and DHEAS levels in women responders during treatment were significantly lower than those observed in women nonresponders (testosterone, $P=0.007$; DHEA, $P=0.046$; DHEAS, $P=0.029$). When men were included in the analysis, DHEA and DHEAS levels during treatment in the responders ($n=20$) were still significantly lower than in the nonresponders ($n=44$) (DHEA, $P=0.0324$; DHEAS, $P=0.0447$).

DISCUSSION

The present study of androgen levels (testosterone, DHEA, and DHEAS) in advanced NSCLC patients treated with gefitinib monotherapy revealed treatment-related decrease, especially in women who had no smoking history. The clinical response of gefitinib treatment appeared to be correlated with the suppression of the hormone levels.

To our knowledge, there have been no previous reports of effects of gefitinib treatment on levels of androgens in patients, although a number of authors have examined relationships between androgens and activity of the epidermal growth factor network (Klein and Nielsen, 1993; Dammann *et al*, 2000; Torring *et al*, 2003). There is evidence that EGFR expression is involved in prostate cancer development and in progression to androgen independence (Di Lorenzo *et al*, 2002), and an *in vitro* study has provided evidence that androgens increase the EGFR levels in androgen-sensitive prostate cancer cells and that EGFR signaling is essential for androgen-induced proliferation and survival (Torring *et al*, 2003). Although there has been no indication of any relationship between androgens and EGFR in NSCLCs, expression of ARs has been detected in NSCLC cell lines and biopsy samples of primary lung cancers (Kaiser *et al*, 1996). Additionally, expression has been detected more frequently in women with adenocarcinoma, and thus this may be a prognostic factor for use of gefitinib in NSCLCs (Fukuoka *et al*, 2003; Kris *et al*, 2003; Miller *et al*, 2004). The data suggest that there is a correlation between the AR and EGFR functions in lung cancer. In agreement with this hypothesis, our results demonstrated clinical responses to gefitinib treatment to correlate with suppression of androgen levels.

One reason for lower androgen levels in responders than nonresponders might be that smokers are resistant and have higher androgen levels. However, there were no significant difference in smoking history between responders and non-responder in our study and there was no significant difference of the pretreatment levels of androgens between smokers and nonsmokers. On the other hand, gefitinib treatment significantly suppressed androgen levels in women who had no smoking history, but not in smokers. Smoking may disrupt the correlation between EGFR and androgen.

Both gefitinib and androgens are metabolised by CYP3A4/5; therefore, it can be speculated that gefitinib may affect the metabolisms of androgens. On the other hand, there are no direct evidences demonstrating PK interaction between gefitinib and androgens. PK interaction between gefitinib and other drugs metabolised by CY3A4/5 such as docetaxel or irinotecan were reported (Fandi *et al*, 2003; Furman *et al*, 2004). These reports suggested that gefitinib may decrease the clearance of these drugs and it may be due to CYP3A4/5 substrate competition. If there are any PK interactions between gefitinib and androgens, androgens clearance may decrease and androgen levels may increase by gefitinib treatment. However, we showed that gefitinib treatment decreased the levels of androgens and it suggested that the effect may not be due to change of CYP3A4/5 activity.

With single estimations of testosterone and DHEA, it is necessary to take into account the circadian rhythms. In this study, all blood was therefore taken at approximately the same time, that is, between 10:00 and 14:00, although this does not preclude any influence of cycles. On the other hand, several reports have suggested that there is no circadian rhythm for serum DHEAS levels (Molta and Schwartz, 1986; Hall *et al*, 1993; Kos-Kudla *et al*, 2001). Therefore, the differences seen in the DHEAS levels in this study presumably reflect actual effects of gefitinib treatment. This would suggest that the data for the other hormones might also have clinical significance.

In conclusion, the results of the present small, retrospective study indicate that androgen levels in NSCLC patients are affected by gefitinib treatment and that they may be factors determining sensitivity to this chemotherapeutic agent. Further large-scale prospective trials are needed in the future to confirm these results and to examine inter-relationships among androgens, smoking, gefitinib sensitivity, and EGFR mutations.

ACKNOWLEDGEMENTS

A part of this study was supported by Grants-in-Aid for Scientific Research from the Ministry of Education, Culture, Sports, Science, and Technology of Japan, and Grants-in-Aid for Cancer Research from the Ministry of Health, Labour, and Welfare of Japan.

REFERENCES

Beattie CW, Hansen NW, Thomas PA (1985) Steroid receptors in human lung cancer. *Cancer Res* **45**: 4206–4214

Dammann CE, Ramadurai SM, McCants DD, Pham LD, Nielsen HC (2000) Androgen regulation of signaling pathways in late fetal mouse lung development. *Endocrinology* **141**: 2923–2929

Di Lorenzo G, Tortora G, D'Armiento FP, De Rosa G, Staibano S, Autorino R, D'Armiento M, De Laurentiis M, De Placido S, Catalano G, Bianco AR, Ciardiello F (2002) Expression of epidermal growth factor receptor correlates with disease relapse and progression to androgen-independence in human prostate cancer. *Clin Cancer Res* **8**: 3438–3444

Fandi A, Gatzemeier U, Smith R, Averbuch S, Manegold C (2003) Final data from a pilot trial of gefitinib (ZD1839) in combination with docetaxel in patients with advanced or metastatic non-small-cell lung cancer (NSCLC): Safety and pharmacokinetics. *Proc Am Soc Clin Oncol* **22**: 655

Ferlay J, Bray F, Pisani P, Parkin DM (2001) *GLOBOCAN 2000: Cancer Incidence, Mortality and Prevalence Worldwide, Version 1.0 (IARC, CancerBase No. 5)*. Lyon, France: IARC Press

Fukuoka M, Yano S, Giaccone G, Tamura T, Nakagawa K, Douillard J-Y, Nishiwaki Y, Vansteenkiste J, Kudoh S, Rischin D, Eek R, Horai T, Noda K, Takata I, Smit E, Averbuch S, Macleod A, Feyereislova A, Dong R-P, Baselga J (2003) Multi-institutional randomized phase II trial of gefitinib for previously treated patients with advanced non-small-cell lung cancer. *J Clin Oncol* **21**: 2237–2246

Furman WL, Daw NC, Crews KR, Stewart CF, McCarville B, Santana VM, Hawkins D, Rodriguez-Galindo C, Navid F, Houghton PJ (2004) A phase I study of gefitinib and irinotecan (IRN) in pediatric patients with refractory solid tumors. *Proc Am Soc Clin Oncol* **22**: 8521

Hall GM, Perry LA, Spector TD (1993) Depressed levels of dehydroepiandrosterone sulphate in postmenopausal women with rheumatoid arthritis but no relation with axial bone density. *Ann Rheum Dis* **52**: 211–214

Kaiser U, Hofmann J, Schilli M, Wegmann B, Klotz U, Wedel S, Virmani AK, Wollmer E, Branscheid D, Gazdar AF, Havemann K (1996) Steroid-hormone receptors in cell lines and tumor biopsies of human lung cancer. *Int J Cancer* **67**: 357–364

Klein JM, Nielsen HC (1993) Androgen regulation of epidermal growth factor receptor binding activity during fetal rabbit lung development. *J Clin Invest* **91**: 425–431

Kos-Kudla B, Ostrowska Z, Marek B, Ciesielska-Kopacz N, Kudla M, Kajdaniuk D, Siemidska L, Strzelczyk J (2001) Circadian serum levels of dehydroepiandrosterone sulphate in postmenopausal asthmatic women before and after long-term hormone replacement. *Endocr Regul* **35**: 217–222

Kris MG, Natale RB, Herbst RS, Lynch Jr TJ, Prager D, Belani CP, Schiller JH, Kelly K, Spiridonidis H, Sandler A, Albain KS, Cella D, Wolf MK, Averbuch SD, Ochs JJ, Kay AC (2003) Efficacy of gefitinib, an inhibitor of the epidermal growth factor receptor tyrosine kinase, in symptomatic patients with non-small cell lung cancer: a randomized trial. *JAMA* **290**: 2149–2158

Law MR, Cheng R, Hackshaw AK, Allaway S, Hale AK (1997) Cigarette smoking, sex hormones and bone density in women. *Eur J Epidemiol* **13**: 553–558

Lin P, Chang JT, Ko JL, Liao SH, Lo WS (2004) Reduction of androgen receptor expression by benzo[alpha]pyrene and 7, 8-dihydro-9, 10-epoxy-7, 8, 9, 10-tetrahydrobenzo [alpha] pyrene in human lung cells. *Biochem Pharmacol* **67**: 1523–1530

Lynch TJ, Bell DW, Sordella R, Gurubhagavatula S, Okimoto RA, Brannigan BW, Harris PL, Haserlat SM, Supko JG, Haluska FG, Louis DN, Christiani DC, Settleman J, Haber DA (2004) Activating mutations in the epidermal growth factor receptor underlying responsiveness of non-small-cell lung cancer to gefitinib. *N Engl J Med* **350**: 2129–2139

Miller VA, Kris MG, Shah N, Patel J, Azzoli C, Gomez J, Krug LM, Pao W, Rizvi N, Pizzo B, Tyson L, Venkatraman E, Ben-Porat L, Memoli N, Zakowski M, Rusch V, Heelan RT (2004) Bronchioloalveolar pathologic subtype and smoking history predict sensitivity to gefitinib in advanced non-small-cell lung cancer. *J Clin Oncol* **22**: 1103–1109

Molta L, Schwartz U (1986) Gonadal and adrenal androgen secretion in hirsute females. *Clin Endocrinol Metab* **15**: 229–245

Non-Small Cell-Lung Cancer Collaborative Group (1995) Chemotherapy in non-small cell lung cancer: a meta-analysis using updated data on individual patients from 52 randomised clinical trials. Non-small Cell Lung Cancer Collaborative Group. *BMJ* **311**: 899–909

Paez JG, Janne PA, Lee JC, Tracy S, Greulich H, Gabriel S, Herman P, Kaye FJ, Lindeman N, Boggon TJ, Naoki K, Sasaki H, Fujii Y, Eck MJ, Sellers WR, Johnson BE, Meyerson M (2004) EGFR mutations in lung cancer: correlation with clinical response to gefitinib therapy. *Science* **304**: 1497–1500

Pao W, Miller V, Zakowski M, Doherty J, Politi K, Sarkaria I, Singh B, Heelan R, Rusch V, Fulton L, Mardis E, Kupfer D, Wilson R, Kris M, Varmus H (2004) EGF receptor gene mutations are common in lung cancers from 'never smokers' and are associated with sensitivity of tumors to gefitinib and erlotinib. *Proc Natl Acad Sci USA* **101**: 13306–13311

Schiller JH, Harrington D, Belani CP, Langer C, Sandler A, Krook J, Zhu J, Johnson DH (2002) Comparison of four chemotherapy regimens for advanced non-small-cell lung cancer. *N Engl J Med* **346**: 92–98

Torring N, Dagnaes-Hansen F, Sorensen BS, Nexo E, Hynes NE (2003) ErbB1 and prostate cancer: ErbB1 activity is essential for androgen-induced proliferation and protection from the apoptotic effects of LY294002. *Prostate* **56**: 142–149

Trummer H, Habermann H, Haas J, Pummer K (2002) The impact of cigarette smoking on human semen parameters and hormones. *Hum Reprod* **17**: 1554–1559

Wakeling AE, Guy SP, Woodburn JR, Ashton SE, Curry BJ, Barker AJ, Gibson KH (2002) ZD1839 (Iressa): an orally active inhibitor of epidermal growth factor signaling with potential for cancer therapy. *Cancer Res* **62**: 5749–5754

WHO (1979) *World Health Organization: WHO Handbook for Reporting Results of Cancer Treatment*, Vol 48, Geneva, Switzerland: WHO Offset Publication

Lung Cancer (2005) 50, 393–399

ELSEVIER

LUNG CANCER

IASLC

www.elsevier.com/locate/lungcan

Plasma MIP-1β levels and skin toxicity in Japanese non-small cell lung cancer patients treated with the EGFR-targeted tyrosine kinase inhibitor, gefitinib

Hideharu Kimura[a,b], **Kazuo Kasahara**[b], **Masaru Sekijima**[c], **Tomohide Tamura**[d], **Kazuto Nishio**[a,e,*]

[a] *Shien-Lab, National Cancer Center Hospital Tsukiji 5-1-1, Chuo-ku, Tokyo 104-0045, Japan*
[b] *Respiratory Medicine, Kanazawa University Hospital, Takara-machi13-1, Kanazawa, Ishikawa, Japan*
[c] *Mitsubishi Chemical Safety Institute, Ibaraki, Japan*
[d] *Medical Oncology, National Cancer Center Hospital, Japan*
[e] *Pharmacology Division, National Cancer Center Research Institute, Tsukiji 5-1-1, Chuo-ku, Tokyo 104-0045, Japan*

Received 15 March 2005; received in revised form 7 July 2005; accepted 15 July 2005

KEYWORDS
Gefitinib;
EGFR;
MIP-1β;
Cytokine;
Lung cancer;
Skin toxicity

Summary Gefitinib (Iressa®) is an orally active, selective EGFR tyrosine kinase inhibitor that blocks signal transduction pathways. Skin toxicity has been reported to be the major toxicity observed in patients treated with the EGFR-targeted tyrosine kinase inhibitors, such as gefitinib and erlotinib. Although the mechanisms underlying the development of the skin toxicity remain to be precisely clarified, immunological mechanisms are considered to be involved. We examined the correlations between the plasma levels of several cytokines and the risk of development of adverse events, especially skin toxicity, induced by the administration of gefitinib as first-line monotherapy in non-small cell lung cancer (NSCLC) patients.

Paired plasma samples were obtained from a total 28 patients of non-small cell lung cancer; the first before the initiation of gefitinib administration (250 mg/day) (24 patients) and the second 2 or 4 weeks after the initiation of treatment (23 patients). The plasma concentrations of 17 major cytokines were measured using a bead-based multiplex assay. The median concentrations of eight of these cytokines before the start of treatment ranged from 0.06 (IL-5) to 58.26 (MIP-1β) (μg/ml). The concentrations of the remaining nine cytokines were under the detectable limit (<0.01 μg/ml) in more than 50% of the samples. Comparisons of the levels before and after treatment showed no significant differences for any of the cytokines measured.

* Corresponding author. Tel.: +81 3 3542 2511x6143; fax: +81 3 3547 5185.
E-mail address: knishio@gan2.res.ncc.go.jp (K. Nishio).

0169-5002/$ – see front matter
doi:10.1016/j.lungcan.2005.07.012

The MIP-1β levels were significantly lower in the patients with skin toxicity (16/24) as compared with those in the patients not showing any skin toxicity (59.1 ± 10.5 versus 119.0 ± 36.8; $p = 0.042$ by the two-sample t-test). The K-Nearest Neighbor Prediction ($K = 3$) showed the classification rate to be 75% for the prediction sets containing MIP-1β, IL-4 and IL-8. There were no significant associations between the levels of any of the cytokines measured and any other parameters, including the tumor response to the drug. In conclusion, the plasma MIP-1β level may be a useful predictor of the development of skin toxicity in patients receiving gefitinib treatment.

1. Introduction

The epidermal growth factor receptor (EGFR) has been found to be expressed, sometimes strongly, in a variety of solid tumors, including non-small cell lung cancer [1,2]. Recognition of the importance of the EGFR in tumor biology provides the rationale for the development of EGFR-targeted cancer therapies. Gefitinib (''Iressa'', ZD1839) is an orally active, selective EGFR tyrosine kinase inhibitor that blocks signal transduction pathways implicated in the proliferation and survival of cancer cells, and also other host-dependent processes that may promote cancer growth [3–5].

Gefitinib has been approved for use as a second-line drug for the treatment of non-small cell lung cancer in Japan, based on evidence collected from large-scale phase II trials (IDEAL 1 and IDEAL 2) [6,7]. In these studies, the adverse effects of gefitinib were mild as compared with those of other cytotoxic agents, and skin toxicity was the most frequently encountered of the adverse events. In some clinical studies, up to 90% of patients treated with gefitinib were reported to suffer from skin toxicity [8]. In others, development of skin toxicity necessitated the discontinuation of gefitinib treatment in some patients [9,10]. Recent publications have reported the development of skin toxicity in patients treated with the anti-EGFR antibody, cetuximab (''Erbitux'', IMC-C225), as well as in those treated with erlotinib (''Tarceva®'', OSI-774), which is an EGFR-targeted small molecule [11–14]. No clear preventive or curative treatment has been established for such drug-induced skin toxicity.

Cytokines mediate numerous physiological and immune reactions, which influence various biological activities, including tumor activity. Activated macrophages secrete many mediators which regulate host defenses by stimulating cellular immunity. Activated macrophages, which produce cytokines such as interleukin (IL)-12, tumor necrosis factor (TNF)-α and interferon (IFN)-α and IFN-β, are powerful activators of natural killer (NK) cells, which have been reported to exert cytotoxic activity against some tumors [15,16]. In non-small cell lung cancer patients, increased production of cytokines such as IL-2, 6, 8 and 10 has been shown to be associated with the response to treatment and survival [17–21]. Other solid tumors have also been shown to possess the ability to produce multiple cytokines [22–25]. These cytokines may act as autocrine growth factors regulating the proliferation and migration of endothelial, tumor, and immune cells. Correlations have been shown between endogenous cytokine levels and the phenotypic manifestations of cancers and prognosis of patients with solid tumors [24–26]. Skin toxicity is the most frequently encountered toxicity in patients treated with EGFR-targeted agents. Some studies have shown evidence of immune reactions in patients developing such skin toxicity, following the administration of other drugs besides the EGFR-targeted agents. In these studies, the levels of various cytokines were elevated after treatment in patients who showed skin toxicity [27–29].

We hypothesized that the serum levels of cytokines may be correlated with the clinical features of patients treated with gefitinib, including the tumor response and adverse effects, especially skin toxicity. To date, no direct comparisons have been made to determine the correlations between cytokine levels and the phenotypic manifestations in cancer patients treated with gefitinib. To investigate the relationship between the cytokine levels and the phenotypic manifestations of cancer in these patients, we measured the plasma concentrations of various cytokines and investigated the roles of these cytokines in NSCLC patients receiving gefitinib as first-line monotherapy.

2. Materials and methods

2.1. Patients and clinical trials

The present study was carried out as a correlative study in a multicenter clinical phase II trial of gefitinib monotherapy, between October 23, 2002, and August 3, 2003. The study was conducted with the

approval of the appropriate ethical review boards, and in accordance with the recommendations of the Declaration of Helsinki for biomedical research involving human subjects. Twenty-eight Japanese patients with histologically or cytologically proven stage IIIb or IV, chemotherapy-naïve NSCLC were enrolled in this trial. Histological subclassification was carried out according to the World Health Organization (WHO) classification (WHO, 1982). Staging was carried out according to the Fourth Edition of the UICC Tumour Node Metastases (TNM) classification. Gefitinib was administrated orally to all patients at a fixed dose of 250 mg daily. Tumor response was evaluated according to the "Response Evaluation Criteria in Solid Tumours" guidelines [30]. Patients were monitored for adverse events during each cycle of therapy, and these events were graded according to NCI-CTC, version 2.0.

2.2. Plasma collection

Blood samples from the 28 NSCLC patients were collected in heparinized tubes before and 14 or 28 days after the initiation of gefitinib administration. After centrifugation of the blood samples at 500 × *g* for 10 min, plasma samples were carefully collected from the top portion of the separated plasma. The separated plasma samples were stocked at −80 °C until use.

2.3. Cytokine assay

A panel of cytokines was measured in duplicate using the Bioplex protein assay kit (Bio-Rad Laboratories, Hercules, CA), in accordance with the instructions of the manufacturer. All samples were diluted by the addition of an equal amount of saline, and 15 μl of the diluted samples were used for this assay. The assay is a novel multiplexed, particle-based, flow-cytometric assay which utilizes anti-cytokine monoclonal antibodies linked to microspheres incorporating distinct proportions of two fluorescent dyes. The assay was customized to detect and quantify IL-1β, IL-2, IL-4, IL-5, IL-6, IL-8, IL-10, IL-12, IL-13, IL-17, G-CSF, GM-CSF, TNF-α, IFN-γ, monocyte chemotactic protein-1 (MCP-1), and macrophage inflammatory protein-1 beta (MIP-1β). The minimum detectable limit for each of the cytokines was 0.01 μg/ml.

2.4. Statistical analysis

Comparisons of the plasma cytokine levels before and after treatment were carried out with Wilcoxon's signed-rank test, using the Stat View software package (version 5.0, SAS Institute Inc., Cary, NC). The correlations between the cytokine levels and the clinical manifestations were analyzed statistically using the two-sample *t*-test with a random variance model, which was performed using the R software package, version 1.9.0 (The R Foundation, http://www.r-project.org/). The patients were categorized into two groups, depending on the grades of the adverse events (Grade 0 versus >Grade 1). Cytokine values lower than the minimum detectable limit were represented as 0.001 pg/ml. When the significant differences were obtained in the two-sample *t*-test, predictive rates were calculated using the *K*-nearest neighbor prediction analysis ($K = 3$).

3. Results

3.1. Patients

A total 28 patients ware enrolled in this trial. The patients ranged in age from 44 to 87 years, with a median of 64 years, and the male:female ratio was 18:10. Plasma samples were collected before treatment from 24 (85.7%) patients and after treatment from 23 (82.1%) patients. All the patients were evaluated for the presence of drug-related adverse events (Table 1). Skin toxicity was the most frequently encountered drug-related adverse event; 71.4% of the patients receiving gefitinib showed skin toxicity.

3.2. Plasma cytokine levels in the lung cancer patients

The plasma levels of various cytokines in the patients are shown in Table 2. Scatter plots of the levels of individual cytokines are shown in Fig. 1. The levels of IL-2, IL-4, IL-7, IL-12, IL-17, IFN-γ, G-CSF, and GM-CSF in the plasma were lower than the minimal detectable limit (<0.01 μg/ml) in more than 50% of the patients. When the cytokine levels before and after treatment were compared, the MCP-1 levels were significantly higher in the

Table 1 Non-hematological toxicity

	0	1	2	3	4	Percentage of ≧ Grade1
Skin	8	13	5	2	0	71.4
Hepatitis	22	4	1	1	0	21.4
Pneumonitis	25	0	0	3	0	1.1
Diarrhea	18	7	2	1	0	35.7
Nausea	19	7	2	0	0	32.1

NCI-CTC version 2.0.

Table 2 Circulating cytokine levels (pg/ml)

	Pre	Post
Number of patients	24	23
IL-1β	0.09 (0–0.26)	0.02 (0–1.01)
IL-2	0 (0–0)	0 (0–11.58)
IL-4	0 (0–1.45)	0 (0–8.46)
IL-5	0.06 (0–0.85)	0.75 (0.03–1.77)
IL-6	16.45 (9.33–40.61)	23.01 (12.17–44.76)
IL-7	0 (0–0)	0 (0–1.88)
IL-8	7.41 (0–17.29)	8.1 (0–27.45)
IL-10	0.63 (0.11–1.65)	1.13 (0.39–1.96)
IL-12	0 (0–0)	0(0–0)
IL-13	0.24 (0–2.01)	1.21 (0–4.69)
IL-17	0 (0–0)	0 (0–0)
IFN-γ	0 (0–1.05)	0 (0–14.01)
TNF-α	0.74 (0–1.91)	1.02 (0.07–3.04)
G-CSF	0 (0–17.61)	0 (0–0)
GM-CSF	0 (0–0)	0 (0–0)
MCP-1[a]	0 (0–20.82)	37.45 (0–51.62)
MIP-1β	58.26 (25.49–95.0)	55.71 (32.65–121.42)

Values are expressed as median (interquartile range).
[a] Significant difference between pre and post.

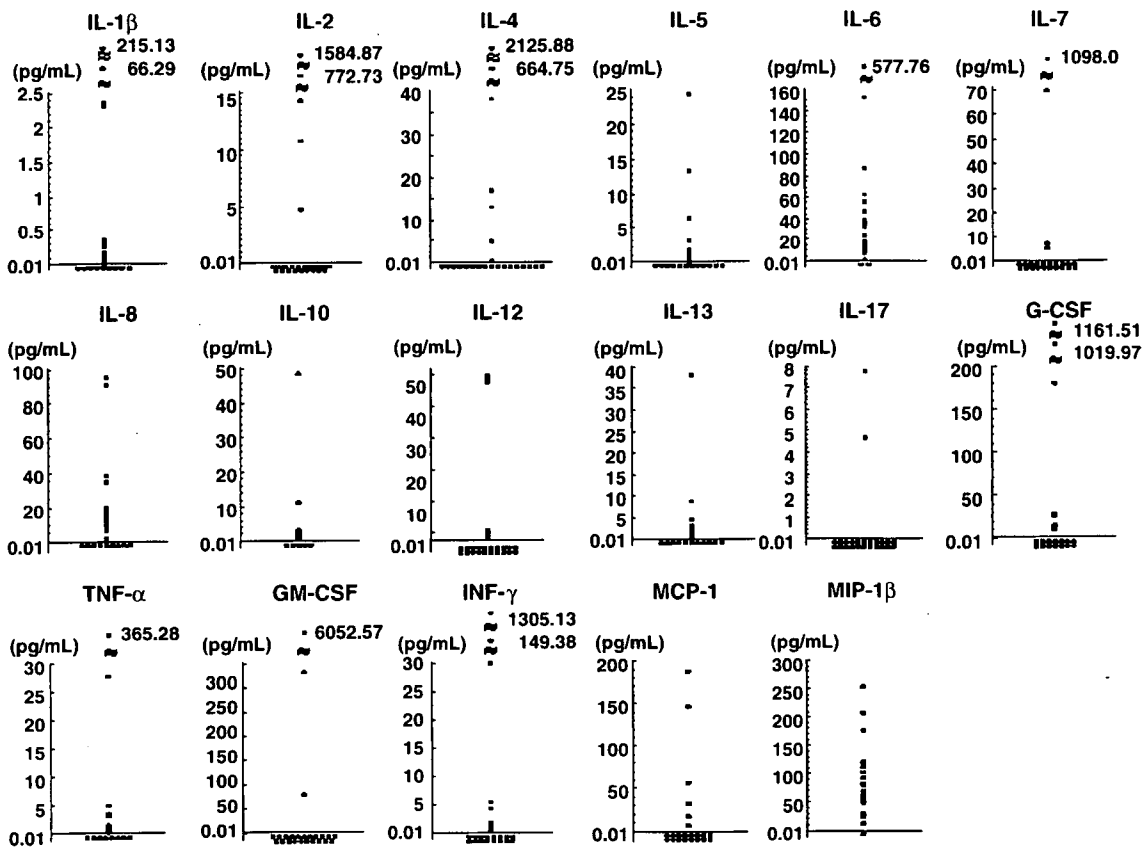

Fig. 1 Plasma concentrations of seventeen cytokines before the commencement of gefitinib in 24 patients. The plots under the line of 0.01 indicate levels lower than the measurement sensitivities.

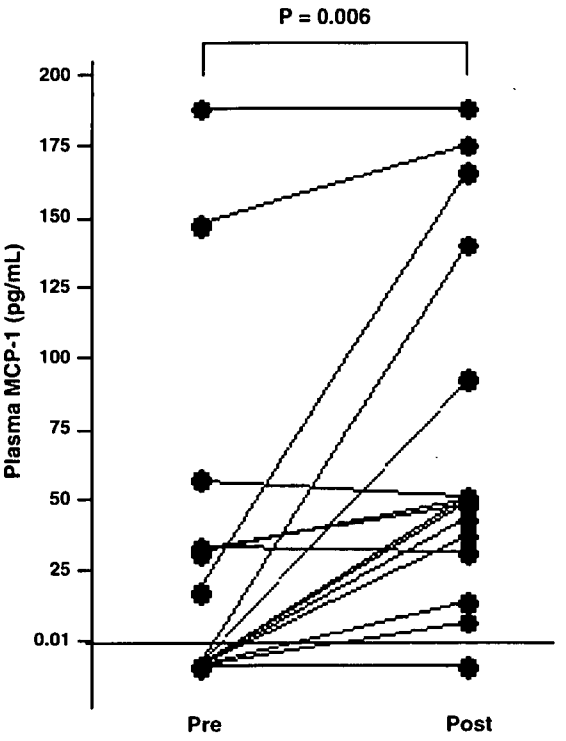

Fig. 2 Plasma concentrations of MCP-1 in 23 patients before and after gefitinib treatment. The differences between the values before and after treatment were significant ($p < 0.05$, paired t-test).

samples obtained after treatment than in those obtained before treatment ($p = 0.006$, by t-test, Fig. 2). There were no significant differences in the levels of any of the other cytokines measured.

3.3. Correlations between cytokine levels and the pharmacodynamic effects of gefitinib

The correlations between the cytokine levels and the clinical features of the patients, including the tumor response, symptomatic improvement, and the development of adverse events, were investigated using the two-sample t-test with a random variance model. There was no significant association between the levels of the various cytokines and the tumor response and symptomatic improvement in any of the patients. When the cytokine levels were comparatively analyzed depending on the grade of adverse events, the patients with skin toxicity (≧ Grade 1) showed significantly lower levels of MIP-1β as compared with those without skin toxicity (Grade 0) ($p = 0.042$, by two-sample t-test, Fig. 3). There was also a trend towards lower levels of IL-8 and IL-4, although the differences were not significant. In addition, the K-nearest neighbor prediction analysis ($K = 3$) showed the classification

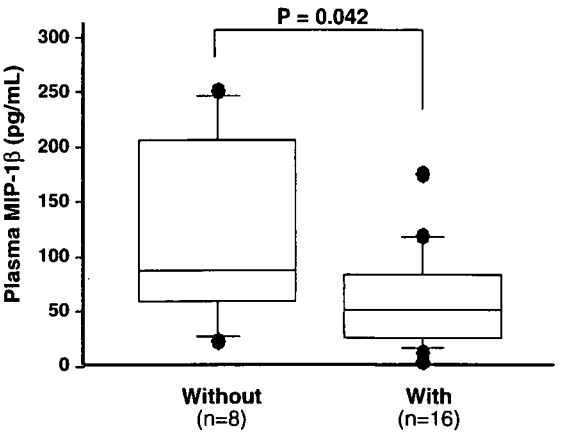

Fig. 3 Box-plots comparing the plasma concentrations of MIP-1β between patients with and without dermatitis; these samples were collected before the initiation of gefitinib. The patients were separated into two groups according to whether or not they developed dermatitis. Patients with skin toxicity showed significantly lower levels of MIP-1β as compared with those without skin toxicity ($p = 0.042$). The top and bottom quartiles and the mean values are depicted as box-plots. Bars indicate the 5th and 95th percentiles of the MIP-1β values.

rate to be 75% for the prediction sets containing MIP-1β, IL-4, and IL-8. There were no significant associations between the cytokine levels and any other parameters.

4. Discussion

The results of this study suggest that a correlation might exist between the serum levels of MIP-1β and the risk of development of skin toxicity during gefitinib administration, with lower levels of the cytokine being associated with a higher risk of appearance of the skin toxicity.

Skin toxicity has been reported to occur commonly in patients treated with EGFR-targeted agents, such as gefitinib, elrotinib, and cetuximab [6–14]. Numerous clinical studies have shown that skin toxicity is more frequently observed as compared to other toxicities during the administration of these drugs. Some studies have described the two major histological findings of the skin toxicity, as follows: presence of keratin plugs with microorganisms in dilated infundibula, and, purulent folliculitis surrounded by an infiltrate composed of lymphocytes and histiocytes, with the superficial portions of some follicles showing dense infiltration with neutrophilic granulocytes [9,31]. The skin toxicity induced by gefitinib has been reported to be similar to that induced by other EGFR-targeted agents, and is believed to result from direct

interference by the drug of the functions of EGFR signaling in the skin [32]. Since the blood levels of cytokines generally reflect the status of immune responses, these histological findings may suggest that the skin toxicity would be correlated with the plasma levels of some cytokines. On the other hand, in normal human skin, EGFR is expressed in the basal epidermal keratinocytes, sweat gland apparatus, and the hair follicle epithelium [33,34]. Therefore, the skin toxicity appears to be related to the mechanism of action of the EGFR-targeted agents and not to allergic reactions [35,36]. These characteristic changes, such as acneform eruptions and skin rashes, are probably secondary to an aberrant differentiation of suprabasal keratinocytes caused by EGFR inhibition.

The results in this study that lower level of plasma MIP-1β were correlated with skin toxicities. MIP-1β is a cysteine–cysteine chemokine that plays a role in inflammation and host defense mechanisms by interacting with its specific receptor CCR1, CCR5 and CCR8 [37,38]. MIP-1β is produced by monocytes, macrophages, lymphocytes and other cell types [39]. MIP-1β is closely related with inflammatory and immune responses. Then, we can arise two possible explanations to our evidence. Immune responses mediated by MIP-1β may play a rule in the healing process of keratinocytes damaged by EGFR-targeted agents. Another is that MIP-1β or its related factors may weaken the inhibiting power of the EGFR-targeted agents, although there is no supporting data for the speculations. Further studies are necessary to clarify the role of MIP-1β for cutaneous reactions.

In this study, 17 kinds of cytokine levels were measured using the bead-based multiplex assay. All of the cytokines were measurable with high sensitivity at once using 15 μl plasma sample volume. It is often difficult to obtain the tumor samples from the advanced non-small cell lung cancer patients. Then, the bead-based multiplex assay might be a useful assay system for biomarkers. This assay system is also able to be customized to detect phosphoproteines such as EGFR and ERK1/2 for the predictive marker for clinical response as the next step.

In conclusion, our results indicate that the plasma MIP-1β level may be a useful predictor of the risk of skin toxicity induced by EGFR-specific tyrosine kinase inhibitors.

Acknowledgements

H. Kimura received support from an Awardee of the Research Resident Fellowship from the Foundation for Promotion of Cancer Research (Japan) for the 3rd Term Comprehensive 10-Year-Strategy for Cancer Control.

References

[1] Salomon DS, Brandt R, Ciardiello F, Normanno N. Epidermal growth factor-related peptides and their receptors in human malignancies. Crit Rev Oncol Hematol 1995;19:183–232.

[2] Franklin WA, Veve R, Hirsch FR, Helfrich BA, Bunn Jr PA. Epidermal growth factor receptor family in lung cancer and premalignancy. Semin Oncol 2002;29:3–14.

[3] Ciardiello F, Caputo R, Bianco R, Damiano V, Pomatico G, De Placido S, et al. Antitumor effect and potentiation of cytotoxic drugs activity in human cancer 15 cells by ZD1839 (Iressa), an epidermal growth factor receptor-selective tyrosine kinase inhibitor. Clin Cancer Res 2000;6:2053–63.

[4] Moasser MM, Basso A, Averbuch SD, Rosen N. The tyrosine kinase inhibitor ZD1839 (''Iressa'') inhibits HER2-driven signaling and suppresses the growth of HER2-overexpressing tumor cells. Cancer Res 2001;61:7184–8.

[5] Koizumi F, Kanzawa F, Ueda Y, Koh Y, Tsukiyama S, Taguchi F, et al. Synergistic interaction between the EGFR tyrosine kinase inhibitor gefitinib (''Iressa'') and the DNA topoisomerase I inhibitor CPT-11 (irinotecan) in human colorectal cancer cells. Int J Cancer 2004;108:464–72.

[6] Fukuoka M, Yano S, Giaccone G, Tamura T, Nakagawa K, Douillard JY, et al. Multi-institutional randomized phase II trial of gefitinib for previously treated patients with advanced non-small-cell lung cancer. J Clin Oncol 2003;21:2237–46.

[7] Kris MG, Natale RB, Herbst RS, Lynch Jr TJ, Prager D, Belani CP, et al. Efficacy of gefitinib, an inhibitor of the epidermal growth factor receptor tyrosine kinase, in symptomatic patients with non-small cell lung cancer: a randomized trial. J Am Med Assoc 2003;290:2149–58.

[8] Dawson NA, Guo C, Zak R, Dorsey B, Smoot J, Wong J, et al. A phase II trial of gefitinib (Iressa, ZD1839) in stage IV and recurrent renal cell carcinoma. Clin Cancer Res 2004;10:7812–9.

[9] van Doorn R, Kirtschig G, Scheffer E, Stoof T, Giaccone G. Follicular and epidermal alterations in patients treated with ZD1839 (Iressa), an inhibitor of the epidermal growth factor receptor. Br J Dermatol 2002;147:598–601.

[10] Jacot W, Bessis D, Jorda E, Ychou M, Fabbro M, Pujol JL, et al. Acneiform eruption induced by epidermal growth factor receptor inhibitors in patients with solid tumours. Br J Dermatol 2004;151:238–41.

[11] Saltz LB, Meropol NJ, Loehrer PJ, Needle MN, Kopit J, Mayer RJ. Phase II trial of cetuximab in patients with refractory colorectal cancer that expresses the epidermal growth factor receptor. J Clin Oncol 2004;22:1201–8.

[12] Govindan R. Cetuximab in advanced non-small cell lung cancer. Clin Cancer Res 2004;10:4241S–4S.

[13] Soulieres D, Senzer NN, Vokes EE, Hidalgo M, Agarwala SS, Siu LL. Multicenter phase II study of erlotinib, an oral epidermal growth factor receptor tyrosine kinase inhibitor, in patients with recurrent or metastatic squamous cell cancer of the head and neck. J Clin Oncol 2004;22:77–85.

[14] Pérez-Soler R, Chachoua A, Hammond LA, Rowinsky EK, Huberman M, Karp D, et al. Determinations of tumor response and survival with erlotinib in patients with non-small cell lung cancer. J Clin Oncol 2004;22:3238–47.

[15] Koh YC, Yuan D. The effect of NK cell activation by tumor cells on antigen-specific antibody responses. J Immunol 1997;139:4745–52.
[16] Lejeune FJ, Ruegg C, Lienard D. Clinical applications of TNF-alpha in cancer. Curr Opin Immunol 1998;10:57380.
[17] McKeown DJ, Brown DJ, Kelly A, Wallace AM, McMillan DC. The relationship between circulating concentrations of C-reactive protein, inflammatory cytokines and cytokine receptors in patients with non-small-cell lung cancer. Br J Cancer 2004;91:1993–5.
[18] Neuner A, Schindel M, Wildenberg U, Muley T, Lahm H, Fischer JR. Prognostic significance of cytokine modulation in non-small cell lung cancer. Int J Cancer 2002;101:287–92.
[19] De Vita F, Orditura M, Auriemma A, Infusino S, Roscigno A, Catalano G. Serum levels of interleukin-6 as a prognostic factor in advanced non-small cell lung cancer. Oncol Rep 1998;5:649–52.
[20] Orditura M, De Vita F, Catalano G, Infusino S, Lieto E, Martinelli E, et al. Elevated serum levels of interleukin-8 in advanced non-small cell lung cancer patients: relationship with prognosis. J Interferon Cytokine Res 2002;22:1129–35.
[21] Hidalgo GE, Zhong L, Doherty DE, Hirschowitz EA. Plasma PGE-2 levels and altered cytokine profiles in adherent peripheral blood mononuclear cells in non-small cell lung cancer (NSCLC). Mol Cancer 2002;1:5.
[22] Steube K, Meyer C, Drexler H. Secretion of functional hematopoietic growth factors by human carcinoma cell lines. Int J Cancer 1998;78:120–4.
[23] Bronte V, Chappell D, Apolloni E. Unopposed production of granulocyte-macrophage colony stimulating factor by tumor inhibits CD8+ T cell responses by dysregulating antigen-presenting cell maturation. J Immunol 1999;162:5728–37.
[24] Chopra V, Dinh T, Hannigan EV. Angiogenin, interleukins, and growth factor levels in serum of patients with ovarian cancer. Correlation with angiogenesis. Cancer J Sci Am 1996;2:279–85.
[25] Chopra V, Dinh T, Hannigan E. Circulating serum levels of cytokines and angiogenic factors in patients with cervical cancer. Cancer Invest 1998;16:152–9.
[26] Pekarek L, Weichselbaum R, Beckett M, Nachman J, Schreiber H. Footprinting of individual tumors and their variants by constitutive cytokine expression patterns. Cancer Res 1993;53:1978–81.
[27] Hertl M, Merk HF. Lymphocyte activation in cutaneous drug reactions. J Invest Dermatol 1995;105:95S–8S.
[28] Hari Y, Urwyler A, Hurni M, Yawalkar N, Dahinden C, Wendland T, et al. Distinct serum cytokine levels in drug- and measles-induced exanthema. Int Arch Allergy Immunol 1999;120:225–9.
[29] Torres MJ, Corzo JL, Leyva L, Mayorga C, Garcia-Martin FJ, Antunez C, et al. Differences in the immunological responses in drug- and virus-induced cutaneous reactions in children. Blood Cells Mol Dis 2003;30:124–31.
[30] Therasse P, Arbuck SG, Eisenhauer EA, Wanders J, Kaplan RS, Rubinstein L, et al. New guidelines to evaluate the response to treatment in solid tumors. European Organization for Research and Treatment of Cancer, National Cancer Institute of the United States, National Cancer Institute of Canada. J Natl Cancer Inst 2000;92:205–16.
[31] Busam KJ, Capodieci P, Motzer R, Kiehn T, Phelan D, Halpern AC. Cutaneous side-effects in cancer patients treated with the antiepidermal growth factor receptor antibody C225. Br J Dermatol 2001;144:1169–76.
[32] Lee MW, Seo CW, Kim SW, Yang HJ, Lee HW, Choi JH, et al. Cutaneous side effects in non-small cell lung cancer patients treated with Iressa (ZD1839), an inhibitor of epidermal growth factor. Acta Derm Venereol 2004;84:23–6.
[33] Nanney LB, Maglid M, Stoscheck CM, King Jr LE. Comparison of epidermal growth factor binding and receptor distribution in normal human epidermis and epidermal appendages. J Invest Dermatol 1984;83:385–93.
[34] Nanney LB, Stoscheck CM, King Jr LE, Underwood RA, Holbrook KA. Immunolocalization of epidermal growth factor receptors in normal developing human skin. J Invest Dermatol 1990;94:742–8.
[35] Herbst RS, LoRusso PM, Purdom M, Ward D. Dermatologic side effects associated with gefitinib therapy: clinical experience and management. Clin Lung Cancer 2003;4:366–9.
[36] Jost M, Kari C, Rodeck U. The EGF receptor, an essential regulator of multiple epidermal functions. Eur J Dermatol 2000;10:505–10.
[37] Premack BA, Schall TJ. Chemokine receptors: gateways to inflammation and infection. Nat Med 1996;2:1174–8.
[38] Bernardini G, Hedrick J, Sozzani S, Luini W, Spinetti G, Weiss M, et al. Identification of the CC chemokines TARC and macrophage inflammatory protein-1 beta as novel functional ligands for the CCR8 receptor. Eur J Immunol 1998;28:582–8.
[39] Matsukawa A, Hogaboam CM, Lukacs NW, Kunkel SL. Cytokines and innate immunity. Rev Immunogenet 2000;2:339–58.